

Air Force Institute of Technology

**AFIT Scholar**

---

Theses and Dissertations

Student Graduate Works

---

3-2002

## A Direct Sequence Code-Division Multiple-Access Local Area Network Model

James R. Rapallo Jr.

Follow this and additional works at: <https://scholar.afit.edu/etd>



Part of the [Digital Communications and Networking Commons](#)

---

### Recommended Citation

Rapallo, James R. Jr., "A Direct Sequence Code-Division Multiple-Access Local Area Network Model" (2002). *Theses and Dissertations*. 4460.

<https://scholar.afit.edu/etd/4460>

This Thesis is brought to you for free and open access by the Student Graduate Works at AFIT Scholar. It has been accepted for inclusion in Theses and Dissertations by an authorized administrator of AFIT Scholar. For more information, please contact [richard.mansfield@afit.edu](mailto:richard.mansfield@afit.edu).



**A Direct Sequence Code-Division  
Multiple-Access Local Area Network Model**

THESIS

James R. Rapallo Jr., Captain, USAF

AFIT/GE/ENG/02M-22

DEPARTMENT OF THE AIR FORCE

AIR UNIVERSITY

**AIR FORCE INSTITUTE OF TECHNOLOGY**

Wright-Patterson Air Force Base, Ohio

Approved for public release; distribution unlimited

## Report Documentation Page

<b>Report Date</b> 15 Mar 02	<b>Report Type</b> Final	<b>Dates Covered (from... to)</b> Jun 01 - Mar 02
<b>Title and Subtitle</b> A Direct Sequence Code Division Multiple Access Local Area Network Model	<b>Contract Number</b>	
	<b>Grant Number</b>	
	<b>Program Element Number</b>	
<b>Author(s)</b> Capt James R. Rapallo, Jr., USAF	<b>Project Number</b>	
	<b>Task Number</b>	
	<b>Work Unit Number</b>	
<b>Performing Organization Name(s) and Address(es)</b> Air Force Institute of Technology Graduate School of Engineering and Management (AFIT/EN) 2950 P Street, Bldg 640 WPAFB, OH 45433-7765	<b>Performing Organization Report Number</b> AFIT/GE/ENG/02M-22	
<b>Sponsoring/Monitoring Agency Name(s) and Address(es)</b> AFCA/ITAI ATTN: Mr. Ronald Price 203 Wes Losey St., Rm 1065 Scott AFB, IL 62225	<b>Sponsor/Monitor's Acronym(s)</b>	
	<b>Sponsor/Monitor's Report Number(s)</b>	
<b>Distribution/Availability Statement</b> Approved for public release, distribution unlimited		
<b>Supplementary Notes</b> The original document contains color images.		

**Abstract**

The United States Air Force relies heavily on computer networks for every-day operations. The medium access control (MAC) protocol currently used by most local area (LAN) permits a single station to access the network at a time (e.g. CSMA/CD or Ethernet). This limits network throughput to, at most, the maximum transmission rate of a single node with overhead neglected. Significant delays are observed when a LAN is overloaded by multiple users attempting to access the common medium. In CSMA/CD, collisions are detected and the data sent by the nodes involved are delayed and transmitted at a later time. The retransmission time is determined with a binary exponential back-off-algorithm. Code Division Multiple Access (CDMA) is a technique that increases channel capacity by allowing multiple signals to occupy the same bandwidth simultaneously. Each signal is "spread" through multiplication with a unique pseudo-random code that distinguishes it from all other signals. Upon reception, the signal of interest is "despread" and separated from other incoming signals by multiplying it with the same exact code. With this technique, it is possible for multiple stations to transmit simultaneously with minimal ill effects. A simulation model is developed for a direct sequence spread spectrum CDMA (DS/CDMA) channel that incorporates the effects of multiple access interferers (MAI) having spreading codes from the same or different code families. The model introduces cross-correlation coefficients to calculate the signal-to-interference ratio and determine channel bit error performance. Transmission media attenuation and the near-far effects are accounted for in the model design. The model utility is demonstrated by determining the loss characteristics of a coaxial spread spectrum network. Due to the modular design, other transmission media characteristic can be easily incorporated. A bus network topology is simulated using 10Base2 coaxial cable. The model is compared and validated against a spread spectrum local area network hardware test bed.

**Subject Terms**

CDMA LAN, Code Division Multiple Access Local Area Network, 10Base-2, Spread Spectrum LAN.

**Report Classification**

unclassified

**Classification of this page**

unclassified

**Classification of Abstract**

unclassified

**Limitation of Abstract**

UU

**Number of Pages**

118

The views expressed in this thesis are those of the author and do not reflect the official policy or position of the Department of Defense or the United States Government.

AFIT/GE/ENG/02M-22

A Direct Sequence Code-Division  
Multiple-Access Local Area Network Model

THESIS

Presented to the Faculty of the School of Engineering and Management  
of the Air Force Institute of Technology

Air University

In Partial Fulfillment of the  
Requirements for the Degree of  
Master of Science

James R. Rapallo Jr., B.S.E.E.

Captain, USAF

March, 2002


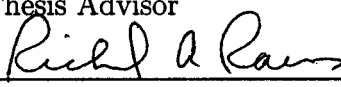
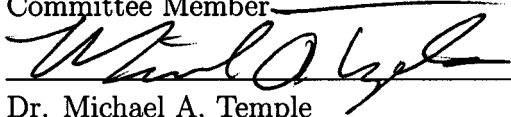
Approved for public release; distribution unlimited

A Direct Sequence Code-Division  
Multiple-Access Local Area Network Model

James R. Rapallo Jr., B.S.E.E.

Captain, USAF

Approved:

	<u>11 Mar 02</u>
Major Rusty O. Baldwin	Date
Thesis Advisor	
	<u>11 Mar 02</u>
Dr. Richard A. Raines	Date
Committee Member	
	<u>11 Mar 02</u>
Dr. Michael A. Temple	Date
Committee Member	

## *Acknowledgements*

I wish to thank my Lord and Savior, Jesus Christ for giving me the strength and encouragement through many obstacles during my studies.

Special thanks are extended to my thesis advisor, Major Rusty Baldwin, whose encouragement and support during this thesis effort was invaluable. Also, to my committee members, Dr. Michael Temple and Dr. Richard Raines, I owe much gratitude for their continued guidance and advice in this research. To James Stephens, thanks for the aid with the lab equipment.

I would like to thank my wife and kids for their sacrifice during my studies. They endured long nights and countless days of whining, kicking, and screaming as I dragged myself back to studies. I thank my wife who bore and reared our new daughter while her husband underwent a lobotomy. Her strength and love kept me going throughout the curriculum.

James R. Rapallo Jr.



## *Table of Contents*

	Page
Acknowledgements . . . . .	iii
List of Figures . . . . .	ix
List of Tables . . . . .	xii
List of Abbreviations . . . . .	xiv
Abstract . . . . .	xvi
I. Introduction . . . . .	1-1
1.1 Background . . . . .	1-1
1.2 Problem and Significance . . . . .	1-2
1.3 Research Goals . . . . .	1-3
1.4 Thesis Organization . . . . .	1-3
II. Literature Review . . . . .	2-1
2.1 Communication Networks . . . . .	2-1
2.1.1 Open Systems Interconnection Reference Model	2-1
2.1.2 Wired and Wireless Networks . . . . .	2-3
2.2 CSMA/CD . . . . .	2-4
2.2.1 Broadband vs. Narrowband . . . . .	2-4
2.2.2 10Base-2 . . . . .	2-5
2.2.3 Ethernet . . . . .	2-5
2.3 Direct Sequenced Spread Spectrum CDMA . . . . .	2-6
2.4 Previous Research . . . . .	2-9

	Page
2.4.1 Performance Analysis of DS/CDMA vs. CSMA/CD LANs . . . . .	2-9
2.5 “Spreadnet” . . . . .	2-13
2.6 Physical Layer Performance . . . . .	2-15
2.6.1 RG-58 Coaxial Cable . . . . .	2-15
2.6.2 Near-Far Effect . . . . .	2-16
2.6.3 Synchronous vs. Asynchronous CDMA . . . . .	2-17
2.6.4 DOCSIS Cable Modems . . . . .	2-18
2.7 Summary . . . . .	2-19
III. Methodology . . . . .	3-1
3.1 Introduction . . . . .	3-1
3.2 Problem Definition . . . . .	3-1
3.3 Research Goals . . . . .	3-2
3.4 Approach . . . . .	3-2
3.5 System Boundaries . . . . .	3-2
3.6 System Services and Possible Outcomes . . . . .	3-4
3.7 Performance Metrics . . . . .	3-4
3.7.1 Simulation Metrics . . . . .	3-4
3.7.2 Test Bed Metrics . . . . .	3-5
3.8 System Parameters . . . . .	3-6
3.8.1 System Parameters . . . . .	3-6
3.9 Factors . . . . .	3-7
3.9.1 Test Bed Factors . . . . .	3-7
3.9.2 Simulation Model Factors . . . . .	3-8
3.10 Evaluation Technique . . . . .	3-9
3.11 Workload . . . . .	3-9
3.11.1 Simulation Model Workload . . . . .	3-9

	Page
3.11.2 Test Bed Workload . . . . .	3-10
3.12 Experimental Design . . . . .	3-10
3.12.1 Simulation Model design . . . . .	3-10
3.12.2 CDMA LAN Test Bed . . . . .	3-14
3.12.3 Experiments . . . . .	3-17
3.12.4 Experimental Error and Normalcy . . . . .	3-18
3.12.5 Verification and Validation . . . . .	3-18
3.13 Summary . . . . .	3-19
IV. Results and Analysis . . . . .	4-1
4.1 Validation of Measurements . . . . .	4-1
4.1.1 Waveplex Board Operation . . . . .	4-1
4.1.2 Measured operational characteristics . . . . .	4-3
4.1.3 3dB Bandwidth Reduction . . . . .	4-6
4.2 DS/CDMA OPNET Model Validation . . . . .	4-7
4.3 Attenuation Experiment . . . . .	4-9
4.3.1 Validation of Analytic Attenuation Model . . . . .	4-9
4.3.2 Spread Spectrum Attenuation . . . . .	4-11
4.4 Bit Error Rate Comparison . . . . .	4-15
4.4.1 Measured Bit Error Rates . . . . .	4-15
4.4.2 ANOVA . . . . .	4-18
4.5 OPNET and Test Bed BER comparison . . . . .	4-20
4.6 Summary . . . . .	4-21
V. Conclusions and Recommendations . . . . .	5-1
5.1 Research Goals . . . . .	5-1
5.2 Results . . . . .	5-1
5.3 Conclusions . . . . .	5-1

	Page	
5.4	Implications and Impact . . . . .	5-2
5.5	Recommendations for Further Work . . . . .	5-3
5.6	Summary . . . . .	5-4
Appendix A.	Data Analysis . . . . .	A-1
A.1	Experiment 1 . . . . .	A-1
	A.1.1 Measurements . . . . .	A-1
	A.1.2 Adjusted Coax Loss Equation . . . . .	A-1
A.2	Experiment 2 . . . . .	A-3
	A.2.1 Measurements . . . . .	A-3
	A.2.2 BER Results with Varied Criteria . . . . .	A-4
	A.2.3 Normality of BER Measurements . . . . .	A-5
A.3	Summary . . . . .	A-7
Appendix B.	Hardware . . . . .	B-1
B.1	Waveplex Spread Spectrum Development Board . . . . .	B-1
B.2	MFJ Cable Analyzer . . . . .	B-3
B.3	New Wave LRS-100 Spread Spectrum Generator . . . . .	B-5
B.4	Hewlett Packard 8568B Spectrum Analyzer . . . . .	B-5
B.5	Hewlett Packard 8645A Agile Function Generator . . . . .	B-6
B.6	Auxiliary Hardware . . . . .	B-6
Appendix C.	OPNET . . . . .	C-1
C.1	OPNET Overview . . . . .	C-1
C.2	Default Pipeline Stages . . . . .	C-2
	C.2.1 Radio Link Transceiver Pipeline . . . . .	C-2
	C.2.2 Bus Link Transceiver Pipeline . . . . .	C-5
C.3	DS/CDMA bus pipeline . . . . .	C-6
C.4	Packet Trace Verification . . . . .	C-8
C.5	Summary . . . . .	C-10

	Page
Appendix D. Setting 6 Analysis . . . . .	D-1
Bibliography . . . . .	BIB-1
Vita . . . . .	VITA-1

## *List of Figures*

Figure		Page
2.1.	The OSI Reference Model . . . . .	2-2
2.2.	Example of a linear feedback shift register [Sk188]. . . . .	2-7
2.3.	Example of signal, $x(t)$ , being spread by code waveform, $g(t)$ , and then despread. . . . .	2-8
2.4.	Diagram of multiple users signal summation with noise. . . . .	2-9
2.5.	Comparison graphs between CSMA/CD and DS/CDMA. . . . .	2-10
2.6.	Capacity analysis of DS/CDMA in regards to BER and with code sequence length equal to 31. [Bon01] . . . . .	2-11
2.7.	Capacity analysis of S/CDMA system [KVM93] . . . . .	2-12
2.8.	Spreadnet Network Interface Block Diagram . . . . .	2-13
2.9.	Near-Far effect illustration. . . . .	2-17
3.1.	Represented system under test. . . . .	3-3
3.2.	Simplified system under test. . . . .	3-3
3.3.	Segmentation of Packets for SNR, BER, and Error Allocation Bookkeeping . . . . .	3-11
3.4.	OPNET model configuration for experiment 2. . . . .	3-15
3.5.	Hardware setup of DS/CDMA LAN test bed for experiment 2. . . . .	3-16
4.1.	Setting 0 Power Spectral Density. . . . .	4-3
4.2.	Setting 1 Power Spectral Density. . . . .	4-4
4.3.	Setting 6 Power Spectral Density (zoomed to center). . . . .	4-5
4.4.	Setting 6 frequency spectrum (full bandwidth). . . . .	4-5
4.5.	3dB Bandwidth measurements for Waveplex Board settings. . . . .	4-6
4.6.	BER curve comparison (a)OPNET calculated BER from SNR and BER curve from actual Q function (b)BER curves with BPSK coherent signalling highlighted [Sk188]. . . . .	4-7

Figure		Page
4.7.	OPNET packet BER curve with calculated BER curve . . . . .	4-8
4.8.	50 foot cable analyzer attenuation measurements and theoretical values. . . . .	4-9
4.9.	100 foot cable analyzer attenuation measurements and theoretical values. . . . .	4-10
4.10.	194 foot cable attenuation measurements and theoretical values. . . . .	4-10
4.11.	Comparison of primary and secondary peak frequency 50-foot attenuations. . . . .	4-12
4.12.	Comparison of primary and secondary peak frequency 100-foot attenuations. . . . .	4-13
4.13.	Comparison of primary and secondary peak frequency 194-foot attenuations. . . . .	4-13
4.14.	Summary of experiment 1 analysis. . . . .	4-14
4.15.	Summary of experiment 1 analysis. . . . .	4-16
4.16.	Measured BER of test bed per trial. . . . .	4-18
A.1.	Adjusted coax loss equation curve compared with 194-foot cable attenuations measured with cable analyzer. . . . .	A-3
A.2.	Bit error measurements for three multiple access interference levels. (a) 4dB MAI level bit error results, (b) 5dB MAI level bit error results, (c) 6dB MAI bit error results. . . . .	A-4
A.3.	(a) Quantile-Quantile Plot for ANOVA normality test, (b) Residual versus Predicted Response for ANOVA independence of errors test. . . . .	A-7
A.4.	Non-zero Quantile-Quantile Plot for ANOVA normality test. . . . .	A-7
B.1.	Waveplex Spread Spectrum Development Board . . . . .	B-2
B.2.	Waveplex Development Board Functional Diagram . . . . .	B-2
B.3.	MFJ-269 Cable Analyzer . . . . .	B-4
B.4.	LRS-100 Spread Spectrum Generator . . . . .	B-5
B.5.	HP 8568B Spectrum Analyzer . . . . .	B-6

Figure		Page
B.6.	HP 8645A Agile Function Generator . . . . .	B-6
B.7.	(a) Telonic step attenuator. (b) Mini-Circuits well balanced mixer and (c) power splitter. . . . .	B-7
C.1.	Radio Link Transceiver Pipeline Execution Sequence for One Transmission [MIL97] . . . . .	C-3
C.2.	Bus Link Transceiver Pipeline Execution Sequence for One Transmission [MIL97] . . . . .	C-6
C.3.	Packet Trace for Verification of DS/CDMA Bus Model . . . . .	C-9



## *List of Tables*

Table		Page
2.1.	Ethernet and IEEE 802.3 1-Mbps and 10-Mbps Network Characteristics . . . . .	2-5
2.2.	RG-58 A/U or C/U characteristics. . . . .	2-16
2.3.	Coaxial cable loss equation legend . . . . .	2-16
3.1.	Transmitted power levels of multiple access interference (assuming no loss) . . . . .	3-7
3.2.	Summary of experiments and related factors. . . . .	3-9
3.3.	Hyperaccess Terminal Settings . . . . .	3-10
4.1.	Spread spectrum transceiver register settings and clock frequencies. . . . .	4-1
4.2.	Settings' theoretical BW, $F_{IF}$ and chip rate. . . . .	4-3
4.3.	Display Settings for Figure 4.2 . . . . .	4-4
4.4.	Display settings for Figure 4.3. . . . .	4-4
4.5.	Display settings for Figure 4.4. . . . .	4-5
4.6.	C.I.s of difference between MFJ measured and theoretical attenuations. . . . .	4-11
4.7.	Summary of data for Figure 4.14 . . . . .	4-15
4.8.	Display settings for Figure 4.15 . . . . .	4-16
4.9.	Analysis of variance of measured bit error rates . . . . .	4-19
4.10.	Summary of Overall BERs for each MAI level. . . . .	4-20
4.11.	BER proportion 90% C.I.s . . . . .	4-20
4.12.	Paired data samples for measured and simulated BER comparison. . . . .	4-20
A.1.	Signal measurements with varied cable lengths for setting 0. . . . .	A-2

Table		Page
A.2.	Signal measurements with varied cable lengths for setting 1. .	A-2
A.3.	BER results using various criteria. . . . .	A-6

## *List of Abbreviations*

### Abbreviation

(A/CDMA)	Asynchronous Code Division Multiple Access
(ACF)	Autocorrelation Function
(AGC)	Auto Gain Control
(AMI)	American Microsystems Incorporated
(ANOVA)	ANalysis Of VAriance
(BER)	Bit Error Rate
(BPSK)	Binary Phase Shift Keying
( $BW_{N-N}$ )	Null-to-Null Bandwidth
(CDMA)	Code Division Multiple Access
(CSMA/CD)	Carrier Sense Multiple Access with Collision Detection
(dBm)	Decibels with reference to 1 milliwatt
(dB)	Decibels
(DOCSIS)	Data Over Cable Service Interface Specifications
(DS/CDMA)	Direct Sequenced Code Division Multiple Access
(DSSS)	Direct Sequence Spread Spectrum
(ETE)	End-to-End
(FDMA)	Frequency Division Multiple Access
(FIFO)	First-In First-Out
(Gbps)	Gigabits per second
(IC)	Integrated Chip
(IF)	intermediate frequency
(LAN)	Local Area Network
(MAC)	Medium Access Control
(MAI)	Multiple Access Interference
(Mbps)	Megabits per second

## Abbreviation

(NIC)	Network Interface Card
(OSI)	Open Systems Interconnection
(PN)	Pseudo-Noise
(PSD)	Power Spectral Density
( $R_c$ )	Chip Rate
( $R_d$ )	Data Rate
(RSA)	Rivest-Shamir-Adleman
(RSSI)	Received Signal Strength Indicator
(S/CDMA)	Synchronous Code Division Multiple Access
(SIL)	Spreadnet Interface Logic
(SIR)	Signal-to-Interference Ratio
(SNL)	Spreadnet Node Logic
(SNR)	Signal-to-Noise Ratio
(SOI)	Signal of Interest
(SS)	Spread Spectrum
(SSART)	Spread Spectrum Asynchronous Receiver and Transmitter
(SSNC)	Spread Spectrum Node Controller
(SWR)	Standing Wave Ratio
(TDA)	Transmission Data Attribute
(TDMA)	Time Division Multiple Access

*Abstract*

The United States Air Force relies heavily on computer networks for everyday operations. The medium access control (MAC) protocol currently used by most local area networks (LAN) permits a single station to access the network at a time (e.g. CSMA/CD or Ethernet). This limits network throughput to, at most, the maximum transmission rate of a single node with overhead neglected. Significant delays are observed when a LAN is overloaded by multiple users attempting to access the common medium. In CSMA/CD, collisions are detected and the data sent by the nodes involved are delayed and retransmitted at a later time. The retransmission time is determined with a binary exponential back-off algorithm.

Code Division Multiple Access (CDMA) is a technique that increases channel capacity by allowing multiple signals to occupy the same bandwidth simultaneously. Each signal is “spread” through multiplication with a unique pseudo-random code that distinguishes it from all other signals. Upon reception, the signal of interest is “despread” and separated from other incoming signals by multiplying it with the same exact code. With this technique, it is possible for multiple stations to transmit simultaneously with minimal ill effects.

A simulation model is developed for a direct sequence spread spectrum CDMA (DS/CDMA) channel that incorporates the effects of multiple access interferers (MAI) having spreading codes from the same or different code families. The model introduces cross-correlation coefficients to calculate the signal-to-interference ratio and determine channel bit error performance. Transmission media attenuation and the near-far effects are accounted for in the model design. The model utility is demonstrated by determining the loss characteristics of a coaxial spread spectrum network. Due to the modular design, other transmission media characteristic can be easily incorporated. A bus network topology is simulated using 10Base2 coaxial

cable. The model is compared and validated against a spread spectrum local area network hardware test bed.

# A Direct Sequence Code-Division Multiple-Access Local Area Network Model

## *I. Introduction*

This chapter provides an introduction to the concepts of Carrier Sense Multiple Access with Collision Detection (CSMA/CD) and the spread spectrum technique of Code Division Multiple Access (CDMA). It presents an overview of the problem at hand, as well as the importance of this problem. Furthermore, it describes each chapter of this thesis.

### *1.1 Background*

The medium access control (MAC) protocol used by most local area networks (LAN) permits a single station to access the network at a time (e.g. CSMA/CD or Ethernet). This limits throughput of the network to, at most, the maximum transmission rate of a single node with overhead neglected. If two or more nodes transmit in the same slot a collision occurs and overall throughput decreases. A LAN is overloaded when multiple users are attempting to access the common medium at once and throughput drops below a certain threshold. In CSMA/CD, collisions are detected and the data sent by the nodes involved are delayed and retransmitted at a later time. The retransmission time is determined with a binary exponential back-off algorithm.

CDMA is a technique that increases channel capacity by allowing multiple signals to simultaneously occupy the same bandwidth. Each signal is “spread” by multiplying it with a pseudo-random noise code that distinguishes it from all other signals. At reception, the signal of interest is “despread” and separated from incoming signals on the channel by multiplying it with the same exact code. With this

technique it is possible for multiple stations to transmit simultaneously without ill effects.

### *1.2 Problem and Significance*

If CSMA/CD could be replaced by CDMA in existing wired LANs, collisions could be virtually eliminated. Each user could fully utilize the maximum bandwidth that the transmission medium supports. Much attention is being focused on incorporating wireless and fibre-optic LANs, but little has been paid to using CDMA in existing infrastructures of coaxial cabling. This research demonstrates that there is much to be gained by doing this.

CDMA allows contentionless access to the network bus. Contentionless access eliminates the need for binary exponential back-off substantially reducing end-to-end delay of packet transmission. Contentionless access also improves network throughput by allowing each user full user-specific bandwidth with immediate and constant access to network. One hundred users transmitting simultaneously at 1 Megabits per second equates to a network throughput of 100 Mbps [SSS87]. Compared to Ethernet, incorporating CDMA into a LAN reduces network end-to-end delay by 850% in overloaded network levels [Bon01]. At the same time, network levels throughput was increased by 250%. These are significant improvements in two very important network performance metrics.

This research investigates the possibility of drastically improving LAN performance Air Force wide by simply installing a spread spectrum network card into each computer. Air Force internal communication systems would be improved tremendously for minimal cost since it would not be necessary to change communication infrastructure in any way. Information could be transferred quicker and more efficiently.



### *1.3 Research Goals*

The goal of this research is to build on the foundation of previous studies towards the ultimate implementation of a Direct Sequence Spread Spectrum CDMA wired LAN over existing Ethernet LAN infrastructures. This is accomplished by validating a simulated CDMA 10Base2 LAN against measurements of a constructed CDMA LAN hardware test bed. Bit-error-rate performance is compared as well as attenuation properties of 10Base2 coaxial cable.

### *1.4 Thesis Organization*

This chapter gives a brief overview of the subject area and the basic goals and direction of the research. Chapter 2 reviews current literature and research on Direct Sequence Spread Spectrum, CDMA, CSMA/CD, coaxial cable properties and previous research in the subject area. It highlights recent advances in each of these areas. Chapter 3 presents the methodology used to accomplish this research including the system definition, evaluation techniques and experimental design. Chapter 4 presents the results and analysis of the experiments and this research. Chapter 5 summarizes and presents conclusions of this research effort.

## II. Literature Review

This chapter presents background information about direct sequenced spread spectrum (DSSS) and applying that to an existing Ethernet local area network (LAN) using RG-58 (*thinnet*) coaxial cable. It presents a basic discussion of network layers, specifically the data link/medium access control (MAC) layer and the physical layer. It provides background on the specific MACs: carrier sense multiple access with collision detection (CSMA/CD) and code division multiple access using direct sequence spread spectrum (DS/CDMA) or (CDMA). CDMA can be further divided into two transmission types synchronous (S/CDMA) and asynchronous (A/CDMA). This chapter also presents previous research supporting the application of CDMA to LANs. Finally, it discusses current application and performance analysis of these topics.

### 2.1 Communication Networks

Communication networks are a valuable commodity in today's United States Air Force. The USAF LAN infrastructure is dominated by the Ethernet protocol over RG-58 10BASE-2 ("thinnet") cable due to its inexpensiveness and ability to utilize BNC connectors that form T-junctions [Hel98]. With the advent of Fast Ethernet (100 Megabits per second (Mbps) throughput) and Gigabit Ethernet (1 Gigabits per second (Gbps) throughput), the 10Mbps throughput that *thinnet* supports is fast becoming obsolete. However, in order to upgrade to the faster throughputs cabling must be replaced. There is substantial cost in replacing infrastructure cabling in a finished building. This research concentrates on improving LAN performance in way that does not require cable replacement.

*2.1.1 Open Systems Interconnection Reference Model.* The International Standards Organization provides a framework for a network. This framework is

called the Open Systems Interconnection (OSI) reference model and describes seven layers that define the communication process in a network (c.f., Figure 2.1).

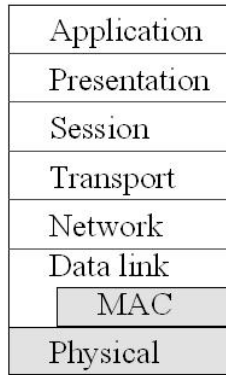


Figure 2.1 The OSI Reference Model

Of the seven OSI layers, this research concentrates on the lower two, the data link and physical layers. The seven layers are described below [Tan96]:

1. The *physical layer* consists of the electrical and physical connection between devices. This layer specifies the cable connections and the electrical rules necessary to transfer data between devices. It specifies characteristics like the length of the coaxial cable, attenuation of the cable and how many and what kind of connections are used to tap into the cable.
2. The *datalink layer* determines how a device gains access to the medium specified in the physical layer, e.g., coaxial cable. It also defines data formats, including the framing of data within transmitted messages or packets, error control procedures, and other link control activities. This layer is responsible for the reliable delivery of information and the correcting or masking of errors. It also contains the medium access control sublayer, which controls how multiple nodes transmit over a common medium.
3. The *network layer* is concerned with routing data packets from source to destination.

4. The *transport layer* accepts data from the session layer and packages it, usually in smaller pieces, in preparation for delivery to the network layer.
5. The *session layer* allows different machines to establish session between each other. The session facilitates two-way communication. The layer is also responsible for keeping synchronization needed for long file transfers.
6. The *presentation layer* converts the network data to data that is compatible with the receiving machine, i.e., converting Unicode to ASCII characters, 1's complement to 2's complement integers, and so on.
7. The application layer is the layer where the data is viewed and used, such as electronic mail, web browsers, etcetera.

*2.1.2 Wired and Wireless Networks.* Wireless networks are rapidly growing in computer industry [Tan96]. The wired network, however, is still dominant in many corporate infrastructures. Bandwidth allocations for the wireless medium differ greatly due to the Federal Communication Commissions frequency allocations. A given radio transmitter is allocated specific bandwidth since it shares the same medium (air) with other transmitters. Wired networks (e.g. coaxial cable), on the other hand, do not share their medium so the total capacity is available. Spread spectrum CDMA is a common multiple access technique in today's digital cellular systems. Time and frequency division multiple access (TDMA)(FDMA) are widely used. Spread spectrum CDMA is the predominant method for transmission and multiple access in 3rd-generation cellular systems. Wireless LAN's are integrating Spread Spectrum into their physical medium but continue to operate with TDMA MAC [IEE97].

Ethernet (or IEEE 802.3) is a very common network using the CSMA/CD method for MAC protocol. The topologies required and segment lengths are determined by the particular medium chosen. The Ethernet protocol's versatility allows for its implementation on a number of network designs [IEE85].

## 2.2 CSMA/CD

The CSMA/CD access protocol is derived from the slotted ALOHA system built by the University of Hawaii [Tan96]. Ethernet is based on their efforts. The CSMA/CD protocol is a MAC that allows every node to transmit on the medium one at a time, essentially a time-division multiple access (TDMA) system. Each node has dedicated time slots to access a common bus. The bus control is given to a node that successfully transmits without any collisions. Each network node listens to the bus for ongoing transmission. If a node has a packet to transmit, it waits until the bus is at high impedance (no transmission) and then transmits. It is possible for two nodes to transmit at the same time, resulting in a *collision*. When this occurs, both nodes backlog their packet and attempt to retransmit at another randomly determined time.

For Ethernet to operate at the full 10 Mbps, it is necessary for each node to burst data onto the network at the full 10 Mbps rate, even though its own requirements for data transmission may amount to much less. Thus, each node must be capable of transmitting at 10 Mbps [SpS87].

*2.2.1 Broadband vs. Narrowband.* Two signaling methods used by conventional LANs such as Ethernet are broadband and narrowband. In broadband signaling, transmission bandwidth is subdivided into smaller frequency channels creating subchannels that allow concurrent and independent transmission of data. Narrowband LANs use only one channel to transmit data, so there is only one signal on the line at time [Hel98]. Narrowband transmission occurs in a frequency range extending from 0 Hz to some maximum frequency equaling the data rate; this is called baseband signaling, with no carrier used for up-conversion.

While broadband systems modulate the data to transmit an analog signal, baseband can keep the signal in its original digital format. The data are sent in the form of 1's and 0's in a number of different representations including *return*

to zero, non-return to zero, unipolar, and bipolar. However, to eliminate the need for a separate clock channel, the signal is further encoded using methods such as Manchester or Differential Manchester [Tan96].

*2.2.2 10Base-2.* As seen in Table 2.1, the 10Base-2 cable standard has a limitation of 185-meter segment length before a repeater must be inserted to regenerate the signal. On this segment there can be a maximum of 30 nodes (workstations). The standard uses RG-58 A/U or RG-58 C/U coaxial cable. Thus, nodes can be attached directly to the cable or bus using BNC barrel connectors or, more commonly, T-connectors. The cable is routed to each workstation through a T-connector that is attached to a BNC connector on each node's network interface card (NIC) [Hel98].

*2.2.3 Ethernet.* Table 2.1 shows comparisons between different wired 802.3 network media [Hel98]. The table shows the design decisions the network designer must make when choosing a medium for a building's networking infrastructure. The design factors of topology, ease of cable installation, cost, and performance are included in this decision.

Table 2.1 Ethernet and IEEE 802.3 1-Mbps and 10-Mbps Network Characteristics

<b>Operational Characteristics</b>	<b>Ethernet</b>	<b>10BASE-5</b>	<b>10BASE-2</b>	<b>1BASE-5</b>	<b>10BASE-T</b>	<b>10BROAD-36</b>
Operating rate (Mbps)	10	10	10	1	10	10
Access protocol	CSMA/CD	CSMA/CD	CSMA/CD	CSMA/CD	CSMA/CD	CSMA/CD
Type of signaling	Baseband	Baseband	Baseband	Baseband	Baseband	Broadband
Data encoding	Manchester	Manchester	Manchester	Manchester	Manchester	Manchester
Maximum segment length (meters)	500	500	185	250	100	1,800
Stations/segment	100	100	30	12/hub	12/hub	100
Medium	50-ohm coaxial (thick)	50-ohm coaxial (thick)	50-ohm coaxial (thin)	Unshielded twisted pair	Unshielded twisted pair	75-ohm coaxial
Topology	Bus	Bus	Bus	Star	Star	Bus

### 2.3 *Direct Sequenced Spread Spectrum CDMA*

A spread spectrum system is defined as a system fulfilling the following requirements [Sk188]:

1. The signal occupies a bandwidth much in excess of the minimum bandwidth necessary to send the information.
2. Spreading is accomplished by means of a spreading signal, often called a code signal, which is independent of the data.
3. At the receiver, “despreading” (recovering the original data) is accomplished correlating the received signal with a synchronized replica of the spreading signal used to spread the signal at transmission.

Specific benefits of spread spectrum systems include [Sk188]:

1. Interference suppression,
2. Energy density reduction,
3. Fine time resolution,
4. Multiple access (derived from interference suppression),
5. and Privacy.

Of these benefits, this research focuses on interference suppression and multiple access. There are two common types of spread spectrum, direct sequence and frequency hopping. This research focuses on DSSS. Binary Phase Shift Keying (BPSK) is the modulation of choice for DSSS systems for reasons described in [Dix76].

The DSSS signal is composed of a data signal that is mixed with a pseudo-noise (PN) code (also called pseudo-random sequence or code). The code is commonly generated with a multi-stage linear feedback shift register. The feedback “taps” on the shift register dictate the sequence and length of the sequence before it repeats. A tap, or the output, from stage 4 in the shift register shown in Figure 2.2 is modulo-2

added with the output of the second to last stage. Subsequent taps are modulo-2 added to the output of the previous adder on the feedback path [Sk188].

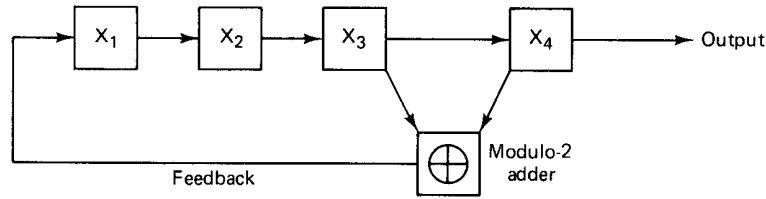


Figure 2.2 Example of a linear feedback shift register [Sk188].

The code is clocked at a faster rate than the data signal. This rate is commonly called the *chipping rate*; for each bit in the code is called a *chip*. The faster chipping rate spreads the frequency spectrum of the narrowband data signal after which the spread signal is transmitted. At the receiver, the signal is despread, demodulated then decoded [Sk188].

The despreading process begins with the synchronization of a local receiver code with the signal. The receiver sends the signal and its spreading code to an auto-correlator that finds a peak auto-correlation power between the two waveforms. When the despreading code is synchronized with the signal, the original data and data rate can be extracted when the two are mixed. Figure 2.3 shows an example of a signal being spread, transmitted, and then despread. The information signal  $x(t)$  is pulsed at 3 time cycles per bit and is 1001 in binary. For this example, the code signal,  $g(t)$ , is pulsed at three times this rate or one time cycle per bit. It is represented as 111100010011 in binary. When the two signals are modulo-2 added (mixing implementations vary) the result is  $x(t)g(t)$ ; this is the transmitted signal's bit pattern. On reception the transmitted signal is auto-correlated, synchronized with the receiver's code,  $g'(t)$ , and the two are modulo-2 added to reproduce the original transmitted information signal,  $x(t)$  [Sk188]. Although the signal is represented here as a bit stream, the signal is commonly transmitted as a BPSK signal. Demodulation transforms the BPSK waveform into data bits that are then decoded.



	T <sub>0</sub>	T <sub>1</sub>	T <sub>2</sub>	T <sub>3</sub>	T <sub>4</sub>	T <sub>5</sub>	T <sub>6</sub>	T <sub>7</sub>	T <sub>8</sub>	T <sub>9</sub>	T <sub>10</sub>	T <sub>11</sub>
x(t)		1			0			0			1	
g(t)	1	1	1	1	0	0	0	1	0	0	1	1
<b>x(t)g(t)</b>	0	0	0	1	0	0	0	1	0	1	0	0
g'(t)	1	1	1	1	0	0	0	1	0	0	1	1
x(t)		1			0			0			1	

Figure 2.3 Example of signal,  $x(t)$ , being spread by code waveform,  $g(t)$ , and then despread.

Multiple access is achieved by choosing distinct spreading codes that have low cross-correlation. That is, if any two codes in the same *code family* are convolved, the resulting value of the convolution is very low. A *code family* is a set of code sequences that are produced from the same implementation (e.g., maximal length sequences and Gold codes). When multiple signals are simultaneously transmitted with different codes of a *code family*, their transmitted power is superimposed on the medium. A receiver wishing to receive a specific code takes the composite signal and correlates it with the desired code. When it has synchronized by detecting a correlation peak, the receiver applies the spreading code and recovers the information signal. Other signals present on the medium will be, in effect, spread even more by this process and their interfering power reduced. This describes the interference suppression attribute of spread spectrum systems. The code sequences should possess the following [SSS87]:

1. Low sidelobe autocorrelation functions (ACF) to permit error free signal acquisition.
2. Low cross-correlation coefficients to maximize the number of simultaneous users by minimizing the cross code interference.

3. Linear spreading function to achieve good spectral spreading.
4. Membership of a large family to provide a large number of orthogonal (or near orthogonal) codes.

Figure 2.4 shows multiple users being added to a channel by mixing their signal with their specific code. Note that noise is also introduced to the integrated signal.

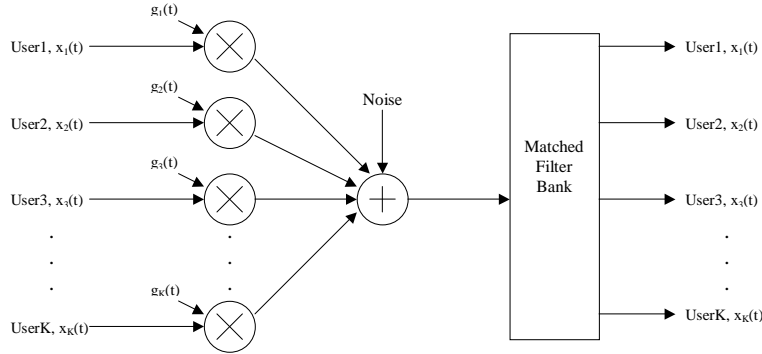


Figure 2.4 Diagram of multiple users signal summation with noise.

## 2.4 Previous Research

The most recent research involved a DS/CDMA MAC over a bus connected LAN is [Bon01]. Bonner conducted a performance analysis between a CSMA/CD LAN and a DS/CDMA LAN and found that in a heavily loaded system overall throughput was much greater in the DS/CDMA LAN. Details of his research are discussed below. Earlier research in this area began in 1983 by Smythe and Spracklen. They built an entire DS/CDMA LAN system for the British Royal Navy [Smy85] [SSS87]. The recent literature will be discussed first.

*2.4.1 Performance Analysis of DS/CDMA vs. CSMA/CD LANs.* Bonner demonstrated that a DS/CDMA LAN impressively outperformed a conventional CSMA/CD LAN [Bon01]. Figure 2.5 shows comparative results in terms of (a) mean throughput, (b) mean delay and (c) mean network power. Power is defined as the ratio of throughput to response time [Jai91].

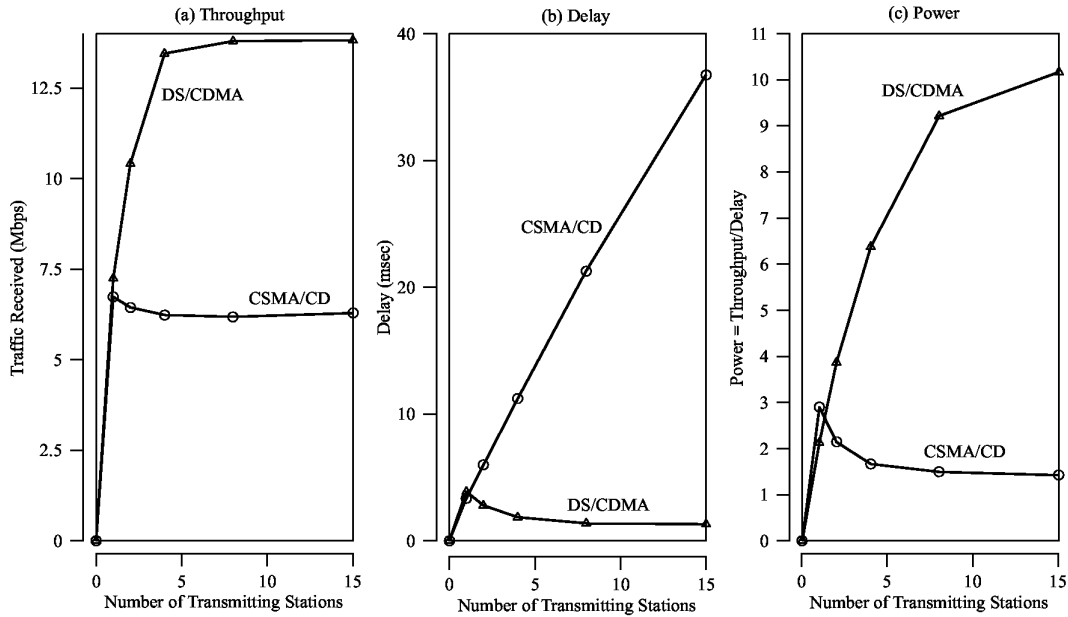


Figure 2.5 Comparison graphs between CSMA/CD and DS/CDMA.

The graphs of Figure 2.5 show that, for a network loading level of 400%, mean throughput and end-to-end (ETE) delay improve by 250% and 850%, respectively. Figure 2.6 shows a capacity analysis in terms of the bit error rate (BER) vs. number of users (stations) transmitting at the same time. These data were found using analytical methods and simulation for a code length of 31 bits. Assuming perfect power control and a code of length 512, up to 98 users could simultaneously transmit on a bus before the signal-to-noise ratio drops to inadequate reception levels, defined as  $10^{-4}$  bit error rates.

Figure 2.6 show the simulation data compared with Gaussian and improved Gaussian approximations for multiple access probability of bit error or bit error rate,  $P_e$ . The Gaussian approximation for  $P_e$  is [LeP87]

$$P_e = Q \left( \frac{k-1}{3N} + \frac{N_0}{2E_b} \right)^{-\frac{1}{2}} \quad (2.1)$$

where  $k$  is the number of simultaneous transmitters,  $N$  is the code length,  $N_0$  is the noise power spectral density, and  $E_b$  is the energy per bit.

## DS/CDMA Validation Plots

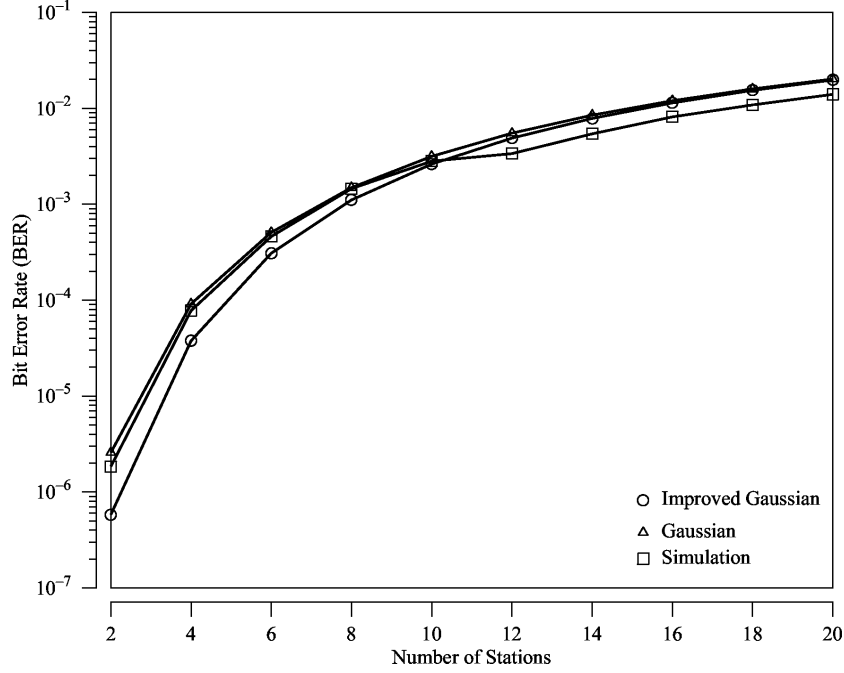


Figure 2.6 Capacity analysis of DS/CDMA in regards to BER and with code sequence length equal to 31. [Bon01]

The improved Gaussian approximation for multiple access  $P_e$  assuming perfect power control is [Hol92]

$$P_e = \left( \begin{array}{l} \frac{2}{3} \left[ Q \left( \frac{k-1}{3N} + \frac{N_0}{2E_b} \right)^{-\frac{1}{2}} \right] \\ + \frac{1}{6} Q \left[ \left( \frac{(k-1)\left(\frac{N}{3}\right) + \sqrt{3}\sigma}{N^2} + \frac{N_0}{2E_b} \right)^{-\frac{1}{2}} \right] \\ + \frac{1}{6} Q \left[ \left( \frac{(k-1)\left(\frac{N}{3}\right) - \sqrt{3}\sigma}{N^2} + \frac{N_0}{2E_b} \right)^{-\frac{1}{2}} \right] \end{array} \right) \quad (2.2)$$

where

$$\sigma^2 = (k-1) \left[ \frac{23N^2}{360} + \left( \frac{1}{20} + \frac{k-2}{36} \right) (N-1) \right] \quad (2.3)$$

Other research analyzes a bipolar synchronous CDMA system's performance using a more generic term, *processing gain*, often denoted as  $M$  or  $G_p$ , as the inde-

pendent variable rather than code lengths. where performance is based on the code family.  $P_e$  for this system is [KVM93]

$$P_e = Q\left(\sqrt{\frac{M}{K-1}}\right) \quad (2.4)$$

where,  $K$ , is the number of simultaneous users and  $Q(x)$  is the complementary error function and defined as [KVM93]

$$Q(x) = \frac{1}{\sqrt{2\pi}} \int_x^\infty \exp\left(-\frac{u^2}{2}\right) du \quad (2.5)$$

The processing gain,  $M$ , is defined as [Sk188]

$$M = \frac{R_c}{R_d} = \frac{T_d}{T_c} \quad (2.6)$$

where  $R_c$  is the chip rate,  $R_d$  the data rate,  $T_c$ , chip duration,  $T_d$  the bit duration. [KVM93] demonstrates that for a  $P_e$  of  $10^{-5}$  a processing gain of 200 is required for the network to accommodate 12 concurrent users. Adding white Gaussian noise to (2.4) will produce the performance in Figure 2.7. These results are much more pessimistic than [Bon01] results in Figure 2.6.

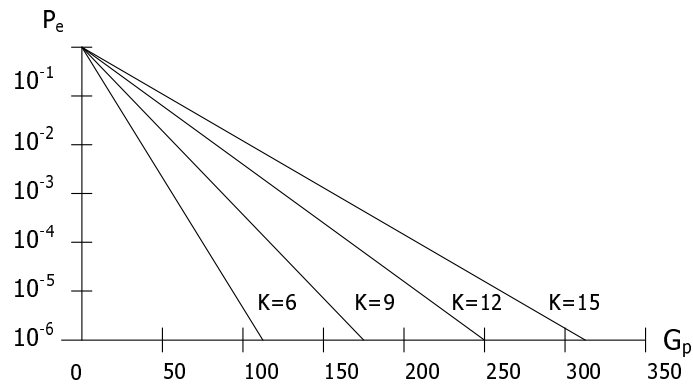


Figure 2.7 Capacity analysis of S/CDMA system [KVM93]

## 2.5 “Spreadnet”

In the early 1980’s, a CDMA wired LAN was built for the United Kingdom Royal Navy named *Spreadnet*. Among the researchers involved were Spracklen and Smythe who wrote a number of papers ranging from 1983 to 1990 recording their progress and documenting lessons learned from this effort. This section presents the system they built and give an overview of their findings [Smy85] [SSS87] [SpS87] [MSS89] [MSS90].

Figure 2.8 shows a block diagram of the NIC used to implement a node’s interface to *Spreadnet*. A workstation contains three components, the Spreadnet Interface

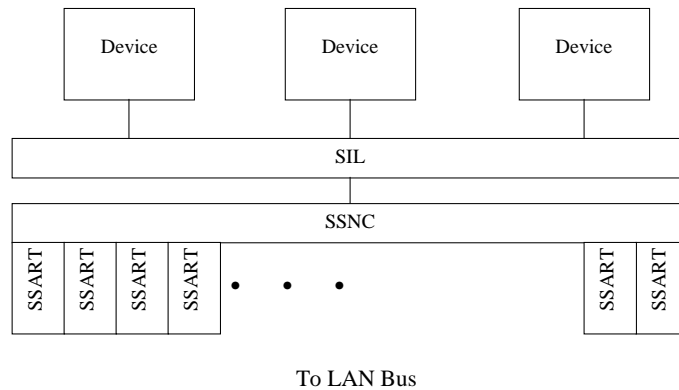


Figure 2.8 Spreadnet Network Interface Block Diagram

Logic (SIL), the Spread Spectrum Node Controller (SSNC) and the Spread Spectrum Asynchronous Receiver and Transmitter (SSART). The last two component form the Spreadnet Node Logic (SNL) [SSS87].

The SIL interfaces the network interface to specific devices enabling them to transmit on the LAN. The SNL module was designed in two sections so that the node could process incoming traffic in parallel while maintaining a flexible interface. The SSNC is responsible for control of the individual nodes and the overall network management, including the distribution of the codes, reconfiguration of the LAN and the logical to physical mapping of user requests to SSART availability. The SSART performs the physical transmission and reception including error de-

tection and correction and correlation and despreading. The arrangement shown in Figure 2.8 allows single or multiple devices, operating in parallel, to communicate with other workstations with unrestricted access to the channel [SSS87].

The DSSS signal is transmitted at baseband and is a digital signal generated from the modulo-2 addition of the PN code and a single data bit. The network has the following properties:

1. Contention-Free Access Mechanism.
2. Transparent Node Addition — Nodes can be added without affecting overall network performance.
3. Decentralization — there is no single point of failure.
4. High Throughput — if one hundred nodes transmit at 1 Mbps then the total throughput is 100 Mbps.
5. Network Resilience — due to the interference suppression attribute of spread spectrum, the network is resilient to many conventionally damaging events (i.e., failure of a single node, burst errors, or noise addition).

The *Spreadnet* system employs dynamic code allocation, which compensates for the fluctuation of the number active nodes on the network. Assuming a constant chipping rate, if more nodes are transmitting, the system will switch to longer PN codes to allow more users to access system, thereby slowing the data rate. When fewer nodes are transmitting, there is less interference and a shorter PN code can be used, thereby increasing the data rate. The system has implicit and explicit security built into it. The implicit security comes from the secure nature of spread spectrum discussed earlier. One must know the individual spreading code to tamper with the transmitted information. The explicit security is the dynamic allocation of spreading codes. When two nodes wish to communicate, the initiator uses the Rivest-Shamir-Adleman (RSA) public key cryptographic algorithm [RSA78] to communicate the PN sequence to be used for the transmissions. Authentication is accomplished using

this method also. A Data Encryption Standard (DES) key is transmitted with RSA and the rest of the communications are encrypted with DES [DES]. These management functions are accomplished on a separate channel to avoid interfering with data traffic.

No detailed performance analysis of the *Spreadnet* system was found. Spracklen and Smythe went on to develop fibre-optic topologies that would allow DS/CDMA operations [MSS89] [MSS90].

## 2.6 Physical Layer Performance

This section discusses the performance aspects of the physical layer as described in the OSI reference model. It presents statistics on the RG-58 coaxial cable (thinnet), reviews an experiment comparing synchronous and asynchronous CDMA and addresses CDMA applications in data over cable service interface specifications (DOCSIS).

*2.6.1 RG-58 Coaxial Cable.* The physical characteristics of coaxial cable, specifically its attenuation properties, can impact the BER performance of a network. Attenuation is signal power loss along the length of a cable. As the signal travels through the cable, a portion of the signal power is converted to heat and a portion leaks through the outer conductor of the cable. Less attenuation is experienced as the size of the cable is increased. Another source of signal loss is signal reflection caused by unmatched impedance along the transmission line [Tim01].

Table 2.2 contains characteristics for the RG-58 coaxial cable currently used in 10Base-2 networks [Tim01].

A coaxial cable power loss equation is [Tim01]

$$A = \frac{0.4343}{Z_o \cdot D} \left[ \frac{D}{d \cdot k_s} + Fbd \right] \cdot \sqrt{F_{MHz}} + \frac{2.78 \cdot df \cdot F_{MHz}}{V_p}. \quad (2.7)$$



Table 2.2 RG-58 A/U or C/U characteristics.

RG-58 Data	
Impedance	50 Ohms
Attenuation – dB/100 ft	
10 MHz	1.416dB
100 MHz	4.566 dB
400 MHz	9.384 dB
1000 MHz	15.3 dB
Frequency Range	0 – 4 GHz nominally
Velocity ratio	.67 (2/3 speed of light)
Impedance	50 Ohms
Resistive loss constant	0.444
Dielectric loss constant	0.00126

Table 2.3 describes the variables in (2.7). The equation can be simplified so the

Table 2.3 Coaxial cable loss equation legend

$A$	Attenuation in dB/100 feet
$Z_o$	Impedance (ohms)
$D$	Dielectric diameter (inches)
$k_s$	1.0 for solid center conductor 0.939 for 7 strand center conductor 0.97 for 19 strand center conductor
$Fbd$	Braid factor
$df$	Dissipation factor
$V_p$	Velocity of propagation (%)
$F_{MHz}$	Frequency (MHz)

coefficients of frequency are reduced to constants,  $k_1$ , the resistive loss constant, and  $k_2$ , the dielectric loss constant, specific for individual types of cable. This is shown in (2.8). Although the equation plots a near linear response to frequency, the actual attenuation in a cable for a given frequency varies with random and periodic cable impedance variations [Tim01].

$$A = k_1 \sqrt{F_{MHz}} + k_2 \cdot F_{MHz} \quad (2.8)$$

*2.6.2 Near-Far Effect.* Attenuation introduces the topic of the *near-far effect*. If Node A in a network is transmitting to a receiver, Node C, at a far distance, the path-loss reduces the received power. If Node B in the network is much closer to the Node C and transmitting with adequate power on the same channel, Node

B could cause enough interference to dominate the channel and drown the signal from Node A. In a spread spectrum system, the signal of interest's (SOI) power is multiplied by the processing gain of the system while the interference is reduced by the cross correlation value. This helps reduce the effect of path loss, but when the SOI is much further away than an interfering node, the interfering node appears as a wideband jammer and the far out SOI is never received. The *near-far effect* is overcome in digital cellular applications by stringent power control algorithms. However, in the digital cellular application there is a single point of reception, the cell tower [PZB95]. This is not so in a LAN. In a LAN there are multiple points of reception and transmission. Figure 2.9 illustrates this example.

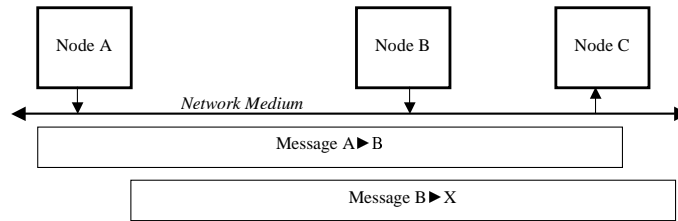


Figure 2.9 Near-Far effect illustration.

One could apply the above example directly to a RG-58 bus network with characteristics of Table 2.2. Suppose Node A was 200 feet away from Node C in Figure 2.9, while Node B was only 100 feet from Node C and both were transmitting at 1 GHz with 40 dB power. Node A's signal reaches Node C with 9.4 dB power, while Node B's reaches Node C with 24.7 dB power. Depending on the CDMA characteristics of the system, Node B's power could prevent acceptable reception of Node A's message.

*2.6.3 Synchronous vs. Asynchronous CDMA.* Most literature addresses CDMA over fiber-optic local area networks as opposed to a coaxial cable LAN. Optical detection systems can only accommodate unipolar signaling as opposed to bipolar signaling in electrical detectors. In [KPP91], an analysis is provided comparing synchronous CDMA (S/CDMA) and asynchronous CDMA (A/CDMA) for a fibre-optic

LAN using a pseudo-orthogonal code sequence that would accommodate optical receivers. Code sequences were generated using prime-length sequences of length  $P$ , with sequence length  $N = P^2$ . One can increase the number of users with S/CDMA by using time-shifted versions of these CDMA code sequences. For A/CDMA the codes must be chosen so that different code phases have a low cross correlation. With S/CDMA one can use this to create more codes with low cross-correlation in a synchronized system. With this code sequence, [KPP91] shows that using S/CDMA the maximum number of subscribers to a system can reach  $P^2$  and the maximum number of simultaneous users,  $K$ , can exceed the number of codes,  $P$ , and maintain an adequate BER. A subscriber is a node that is connected to the LAN, while a user is a node that is transmitting. In fact, as  $N$  increases, it is possible to obtain more users,  $K > P$  and keep a constant BER.

Compared to A/CDMA, S/CDMA provides the following advantages: the system can handle  $P^2$  subscribers as opposed to A/CDMA  $P$  subscribers; S/CDMA can accommodate  $P - 1$  simultaneous users without error, while A/CDMA accommodates less than  $P - 1$  with higher probability for errors (In this code family example,  $P = 31$ , results  $K = 23$  with a BER of  $10^{-9}$ ); and S/CDMA has better performance than A/CDMA as  $P$  increases. A Gaussian approximation for the probability of a bit error,  $P_{e|G}$ , using S/CDMA is [KPP91]:

$$P_{e|G} = \Phi \left( \frac{-P}{\sqrt{K-1}} \right). \quad (2.9)$$

For A/CDMA the approximation is

$$P_{e|G} = \Phi \left( \frac{-P}{\sqrt{1.16(K-1)}} \right) \quad (2.10)$$

where,  $\Phi$ , is the unit normal cumulative distribution function [KPP91].

*2.6.4 DOCSIS Cable Modems.* Spread spectrum techniques described above have been implemented in DOCSIS cable modems in recent years. Terayon Communication Systems has applied this advanced physical layer scheme to upstream transmissions of cable users. They have chosen to use a synchronous variation of CDMA, S/CDMA. They claim that using a synchronized system eliminates interference between codes so more users can be supported by the system. Certain code sequences exist that are completely orthogonal when synchronized. As a result of this orthogonal code set, the cross-correlation between codes is reduced to zero which eliminates interference between codes. Terayon has implemented a backwards-compatible system that allows for CDMA as well as time-division multiple access (TDMA) operation [GRP00].

S/CDMA attempts to eliminate cross-correlation noise that results when using asynchronous CDMA. Multiple waveforms of asynchronously transmitted codes are not aligned or in any desired phase. When each signal is added to the medium, the interference level is raised and capacity is reduced. Codes for asynchronous transmission are chosen to have correlation parameters that are low for any given phase of the code. In S/CDMA, the chips are aligned and the desired phase is captured so that the best possible cross-correlation is achieved. Codes that have a low correlation parameter for a specific phase of the code are chosen for synchronous transmission [MSS90]. This technology allows S/CDMA cable modems to operate below 20 MHz, a region that is off-limits to conventional cable modems due to high noise. It also provides 14 Mbps two-way communication [Rak97].

## *2.7 Summary*

This chapter discusses the present state of communication networks and the OSI layers of networking. A brief review of spread spectrum communications was presented and the concept of using DS/CDMA in the medium access control layer of a local area network was introduced. Prior research in this area was identified.

It presented an understanding of important concepts necessary to consider when implementing a DS/CDMA LAN over a wired network such as the near-far effect and the ability to use S/CDMA transmission in order to lower cross-correlation coefficients and increase capacity in a multi-transmitter environment.

### *III. Methodology*

#### *3.1 Introduction*

This chapter presents the methodology of the experiments for this research. It presents the problem, states the research goals, defines the system under test and the significant parameters of the system. It defines a simulated local area network and a hardware test bed implementation used to validate the LAN. It also presents the experiments that are conducted and the factors that are varied for each experiment.

#### *3.2 Problem Definition*

A characteristic inherent in spread spectrum (SS) systems is the bandwidth used for SS transmission is much greater than the minimum required for data transmission [Skl88]. The multiple access properties of DSSS, when used in a high traffic volume LAN environment, allow DS/CDMA to perform spectacularly since high overall throughput can be obtained as well as low ETE delay [Bon01]. In order to attain comparable data rates, even in a high volume traffic environment, much higher frequencies must be used to sustain long PN codes and high chipping rates with equivalent data rates and achieve low cross-correlation coefficients and high processing gain, respectively. Therefore, in order to accurately model a DS/CDMA LAN, one must consider the undesirable effects of transmitting these higher frequencies over coaxial cable. As shown in the previous chapter, the signal propagation properties of the RG-58 coaxial cable quickly degrade at higher frequencies. The degradation of signal power over variable distances causes a number of problems when implementing such a system as a wired DS/CDMA LAN over a lossy medium. These include the near-far effect and higher bit error rates.

Prior research did not validate the bit error performance of the DS/CDMA model with analytic or real system data due to the absence of a wired LAN implementation of DS/CDMA [Bon01]. In order for further research to conduct valid

capacity analysis on this model, the multiple access interference equations in the model must be incorporated and validated.

### *3.3 Research Goals*

The goals of this research are as follows:

1. To implement a complete model of a DS/CDMA LAN using bus transceiver pipeline from a network simulation tool for future bus architecture analysis.
2. To include 10Base-2 coaxial cable attenuation properties in the model and validate them with hardware measurements.
3. To validate the multiple access interference calculations of the model with BER measurements of a test bed implementation of a DS/CDMA LAN.

### *3.4 Approach*

An American Microsystems Incorporated (AMI) Waveplex spread spectrum transmitter and receiver development board [Wav98] is used to test and measure the parameters, factors and metrics listed herein. The board is included in a CDMA LAN test bed configuration. The measurements obtained are used to validate the outputs of a system modeled with the OPNET V8.0.B network modeling software package [MIL97]. The OPNET model models a variably sized DS/CDMA LAN over 10Base-2 coaxial cable.

### *3.5 System Boundaries*

The focus of this research is on the MAC sublayer and the physical layer of the OSI network model. The system includes multiple stations simultaneously transmitting and receiving over a common 10base-2 coaxial cable bus as shown in Figure 3.1. However, the represented system is simplified by a system including a single receiver and two transmitters shown in Figure 3.2. One transmitter is the

### Represented DS/CDMA LAN System

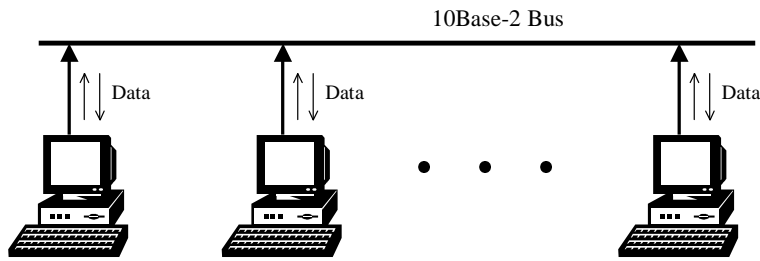


Figure 3.1 Represented system under test.

signal of interest while the other simulates multiple access interference. The receiver acquires data from the signal of interest.

### Simplified DS/CDMA LAN System

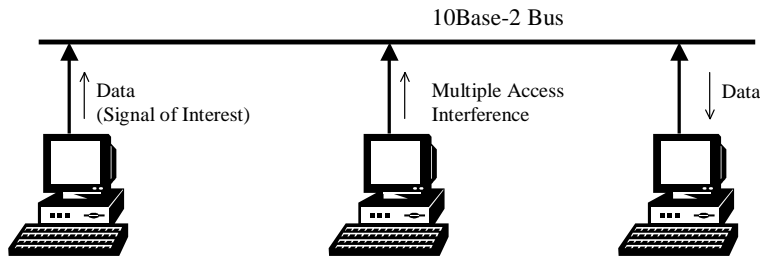


Figure 3.2 Simplified system under test.

The DS/CDMA modeled system includes the following characteristics:

- Each station taps a single bus channel,
- The only interference noise on the network is due to other transmissions,
- Pass band transmission,
- Imperfect power control and
- Perfect synchronization

The system does not include the computer node characteristics, such as processor speed, memory, and disk space. It does not include any functional unit above the MAC sublayer.



### 3.6 System Services and Possible Outcomes

The described system provides communication between multiple stations connected to a common bus topology. The system allows any node to simultaneously and immediately access the bus in order to transmit data. Once the data is transmitted, there are three possible outcomes:

1. The bits arrive correctly,
2. The bits arrive with errors,
3. The bits do not arrive at all.

### 3.7 Performance Metrics

The metrics used to compare the simulation model to the test bed measurements are the bit error rate (BER) and cable attenuation. The metrics and the method of obtaining them are presented separately for the simulation model and the test bed.

*3.7.1 Simulation Metrics.* This section describes the BER metric and its calculation in the simulation model. The BER is defined in BPSK systems as [Sk188]

$$P_b = Q(\sqrt{2E_b/N_o}) \quad (3.1)$$

where  $Q(x)$  is the complementary error function. The complementary function is

$$Q(x) = \frac{1}{\sqrt{2\pi}} \int_x^\infty \exp\left(-\frac{u^2}{2}\right) du \quad (3.2)$$

where  $u$  is the variable of integration. It can be approximated as [BoS79]

$$Q(x) \cong \frac{1}{\sqrt{2\pi}} \cdot \frac{1}{\sqrt{1+x^2}} \exp\left(-\frac{x^2}{2}\right) \quad \text{for } x \geq 0. \quad (3.3)$$

The BER metric takes into account the received bit energy to noise level,  $E_b/N_0$ . The metric describes the quality of signal received in a manner describing the rate at which bits are received in error.

The OPNET model accounts for band pass signaling. The BER can be derived by the calculated signal-to-noise ratio (SNR), or  $\frac{S}{N}$ , at the receiver by first finding the equivalent  $E_b/N_0$  and substituting into (3.3).  $E_b/N_0$  is defined in terms of SNR as [Sk188]

$$\frac{E_b}{N_o} = \frac{S}{N} \left( \frac{W}{R} \right) \quad (3.4)$$

where  $W$  is the receiver's filter bandwidth, and  $R$  is the data rate. A 3dB half-power filter is assumed for the test bed receiver. Calculating the 3dB area under the unit  $\text{sinc}^2(x)$  function results in a  $\frac{W}{R}$  ratio of 0.88. This research approximates this ratio by one. This calculation is shown in Appendix D. Thus, for this research,  $E_b/N_0$  approximately equals SNR. This relationship is verified in Chapter IV by comparing the BER curve created by varied transmission power in OPNET and the known BER curve for BPSK coherent signaling given by (3.1).

Another metric used in the experiments is the power attenuation,  $A$ , from transmitter to receiver in any given pair of nodes. Attenuation is calculated in the simulation model with the coaxial loss equation given in Chapter II.

*3.7.2 Test Bed Metrics.* This section presents the metrics described above and the method of obtaining them from the test bed. The measured BER is

$$BER = \frac{\text{Total Number of Bit Errors}}{\text{Total Number of Bits Transmitted}} \quad (3.5)$$

where bit errors are determined by comparing bits sent and bits received.

Attenuation is measured in terms of transmitted power,  $P_t$ , and received power,  $P_r$ , as

$$A = P_t - P_r \quad (\text{dB}). \quad (3.6)$$

### 3.8 System Parameters

*3.8.1 System Parameters.* The system parameters of interest are:

- Cable length
- Multiple Access Interference (MAI) power
- Cable attenuation (dB/100 ft)
- Cable type: RG-58 A/U (10base-2, “thinnet”) coaxial cable
- Signal of Interest (SOI) Transmit power
- Transmitted null-to-null bandwidth ( $BW_{N-N}$ )
- Modulation: Binary Phase Shift Keying (BPSK)
- Chipping rate,  $R_c$ : 3.05, 5.81, 21.3 MHz
- Data rate,  $R_d$ : 250 Kbps, measured from board.
- Code length: 31 bits
- Code family: maximal length sequences

The transmitted power over the 3dB bandwidth is recorded from the two transmitters for input into the OPNET model simulation. The transmitted power of the interference to the system is a factor. Its levels are listed below in section 3.9. The Waveplex SS board transmits 15.71 milliwatts in the 3dB bandwidth.

Test Bed specific parameters are:

- ASCII file size, 2049 characters. This value was limited by the performance of the Waveplex SS board as described in Appendix B.

- Shift register taps for PN generation: Taps 5,4,2,1 are selected for the PN generator for the interference source, while the spread spectrum board uses taps 5,2.

### 3.9 Factors

This section describes the factors that are to be varied to compare performance between the test bed measurements and the simulation model. The test bed factors and the simulation model are presented separately for clarity of discussion.

#### 3.9.1 Test Bed Factors.

- Interference. Spread spectrum interference is introduced by a BPSK PN sequence generator mixed with a 4.99 MHz signal at a constant power. The power is then attenuated with a decibel step attenuator to produce the power levels listed in Table 3.1. The levels are described as the amount of attenuation in dB of the mixed interference signal from the *raw mixed interference signal* (no attenuation).

Table 3.1 Transmitted power levels of multiple access interference (assuming no loss)

Factor	3dB Bandwidth Power Level (W)
<i>Raw Mixed Interference Signal</i>	0.08354
-4dB	0.03013
-5dB	0.02357
-6dB	0.01836

The power values were calculated in Watts using Parseval's theorem for a real-valued periodic signal, [Hay83]:

$$P_x = \frac{1}{T_0} \int_{-T_0/2}^{T_0/2} x^2(t) dt = \sum_{-\infty}^{\infty} |c_n|^2 \quad (3.7)$$

where the  $c_n$  terms are the complex Fourier series coefficients, or the voltage of each frequency in the spectrum. The power levels were calculated by summing

the square of each voltage in the signal spectrum found with the HP8568B spectrum analyzer. The power levels represent the transmitted power within the signal's 3dB bandwidth. The 3dB bandwidth is chosen to represent the signal strength since it contains most of the signal energy [AMI43].

The -6dB Interference power level, 18.36 mW, when compared to the transmitted power of the Waveplex board, 15.71 mW, provides slightly more power than needed to simulate one additional user on the bus. Likewise, the -4dB interference power level, 30.13 mW, permits the approximation of two multiple access interferers. These factors were chosen to allow a range of BERs to compare with the OPNET model simulation. Any increase in interference power from the -4dB attenuation level caused immediate loss of synchronization.

- Cable length. Three lengths of cable are chosen to test attenuation with a DSSS signal - 50, 100, 194 feet. Smaller lengths of cable are used for connections between mixer and step attenuator. These cables are between two and three feet and are ignored in analysis.
- The chipping rate,  $R_c$ , was chosen as 3.05 MHz and 5.81 MHz (c.f., Appendix D for 21.3 MHz chip rate). We used chipping rates the Waveplex SS board supported.

Since (3.8) describes  $BW_{N-N}$  dependency on the chipping rate ( $R_c$ ), the  $BW_{N-N}$  is also varied accordingly.

$$BW_{N-N} = 2 \cdot R_c \tag{3.8}$$

A summary list of factors and their levels for each experiment is shown in Table 3.2.

*3.9.2 Simulation Model Factors.* This section restates the factors mentioned above as inputted into the OPNET model.

- MAI power. The MAI power levels are given in Watts in Table 3.1.

Table 3.2 Summary of experiments and related factors.

	Interference Power	Cable Length	Chipping Rate
Experiment 1	0	50ft	3.05 MHz
		100ft	5.81 MHz
		194ft	21.3 MHz
Experiment 2	4dB	0ft	5.81 MHz
	5dB		
	6dB		

- Peak power response. It was found that the chipping rates given above produced primary lobe and secondary lobe peak power responses at varied frequencies. These frequencies were used for attenuation comparison. They are 3.99 MHz, 5.1 MHz, 9.391 MHz, 13.69 MHz
- Cable length. The cable lengths used in the model were 50 feet, 100 feet and 194 feet.

### 3.10 Evaluation Technique

We used measurement and simulation. The system is the simulation model, test bed and cable measurements were used to validate the system.

### 3.11 Workload

The experiments require a very basic workload. Since the system boundaries concentrate on the physical layer, the frequency and sustainment of the workload submitted to the system is insignificant. As long as the transmitters are transmitting data constantly and simultaneously on the common bus, the appropriate metrics can be collected.

*3.11.1 Simulation Model Workload.* In the OPNET model, simple sources were modeled that provided each transmitter with constant data flow.

*3.11.2 Test Bed Workload.* The Waveplex spread spectrum board test bed workload is submitted through a terminal emulator interface to the on-board micro-controller chip, which, in turn, submits the data to the on-board transmitter for transmission. The terminal settings used are listed in Table 3.3. An ASCII file was created and repeatedly sent through the terminal to simulate constant data transmission. Non-printable characters are displayed in their hexadecimal form.

Table 3.3 Hyperaccess Terminal Settings

Bits per second	57600
Data bits	8
Parity	None
Stop bits	1
Flow control	None

### *3.12 Experimental Design*

*3.12.1 Simulation Model design.* The initial OPNET model for a DS/CDMA LAN existed from prior research [Bon01]. This research added coaxial attenuation properties and removed perfect power control assumptions from the system in order to validate it against the test bed. This research also modified the model to incorporate a bus architecture rather than a simulated bus with wireless (radio) transmission. Several properties of the OPNET radio model were needed in the bus model, including multiple channels and interference calculations that are not in the default bus model. Thus, the 14 stage OPNET radio model was condensed into the six stage bus model. An in-depth explanation of the OPNET pipeline stages is presented in Appendix C. Highlights of the modifications are presented here.

*3.12.1.1 Attenuation.* Stage 2 of the DS/CDMA bus pipeline model calculates the propagation delay as well as the power presented to the receiver prior to any interference. Perfect power control is negated by including the coaxial loss (2.8) into this stage. The cable attenuation is a function of the frequency of the transmitted signal. The center frequency is chosen to approximate the received

spectrum’s attenuation since most of the signal power is transmitted on either side of the center frequency.

*3.12.1.2 SNR, BER, and Error Allocation.* Unlike the radio pipeline, which has three repeating stages that tracks collisions and multiple access interferers, the bus pipeline only has one repeating stage for this. Thus, sections of SNR, BER and error allocation code were replicated and placed in various pipeline stages to emulate OPNET’s radio model calculations of the same name. Details of OPNET’s transceiver bus and radio pipeline stages are presented in Appendix C.

Figure 3.3 shows the process for SNR, BER and error allocation for the bus transceiver pipeline.

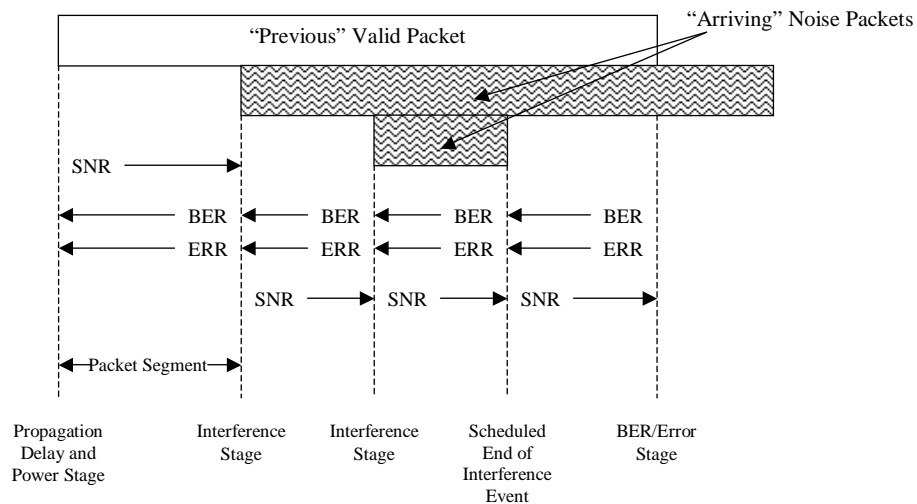


Figure 3.3 Segmentation of Packets for SNR, BER, and Error Allocation Book-keeping

The *Propagation Delay and Power Stage* is the last stage called by OPNET’s kernel before transmission begins. In this stage, the initial SNR (i.e., ambient noise) for a valid packet is calculated. The *Interference Stage* is called at the beginning of reception for each new packet present on the bus. It calculates the BER, allocates errors (ERR) for the preceding valid packet segment, increments the accumulated noise variable for the valid packet and calculates the SNR for the next valid packet



segment. The *Scheduled End of Interference Event* is only scheduled when there is a noise packet that has an end of reception time less than the valid packet's end of reception time. It performs the same bookkeeping functions as the *Interference Stage* except that the accumulated noise variable is decremented because the interfering packet has completed reception. The *Interference Stage* and the *Scheduled End of Interference Event* are called repetitively for as many interfering transmissions that meet the criteria at the beginning and end of the interfering packet, respectively.

*3.12.1.3 Multiple Access Interference.* The accumulated noise calculations are a combination of ambient noise, jamming and multiple access interference. The SNR effectively determines the bit error rate for the system where the signal is attenuated by different noise or interfering sources. The following derivation for the final SNR calculation used in the model accommodates each interference source [Bon01]. In a DSSS BPSK spread spectrum system, the SNR of a signal having average power,  $S$ , in an additive white Gaussian noise channel and average noise power,  $N$ , is

$$SNR_{\text{Despread}} = \frac{S'}{N'} = GP \cdot (SNR) = GP \cdot \left(\frac{S}{N}\right), \quad (3.9)$$

where the primes indicate the spread signal power transmitted and  $GP$  is the processing gain. The next type of interference is multiple access interference (MAI) from another DSSS transmission spreading its data with a code from the same family as the SOI. The cross-correlation coefficient,  $z_{ij}$ , is [Sk188]

$$z_{ij} = \frac{\text{number of digit agreements} - \text{number of digit disagreements}}{\text{total number of digits}} \quad (3.10)$$

where the numerator is called the cross-correlation number and  $i$  and  $j$  are different phases of the code.

The code family used in this research is maximal length sequences. The 31 bit m-sequences used have a maximum cross-correlation number of 9 [AMI43]. Thus, this code family has a maximum cross-correlation coefficient of  $z_{\max} = 0.29$ . The SNR due to MAI or  $SNR_M$  can be calculated as

$$SNR_M = \frac{S'}{M'} = \alpha \cdot GP \cdot \frac{S}{M}. \quad (3.11)$$

where,  $\alpha$ , is a scaling value with some relation to the cross-correlation coefficient of the M-sequences used and represents an expected value of all code phases. All other types of interference are “jamming” sources,  $J(t)$ . The signal-to-jamming ratio is

$$SNR_J = \frac{S'}{J'} = GP_J \cdot \frac{S}{J}. \quad (3.12)$$

Combining the three types of SNR together yields a signal that is attenuated by the sum of each interference called a signal-to-interference ratio (SIR):

$$SIR = \frac{S'}{M' + J' + N'}. \quad (3.13)$$

Substituting (3.9), (3.11) with the  $\alpha$  value, and (3.12) into (3.13) yields:

$$SIR = \frac{(GP)S}{N + \left(\frac{GP}{GP_J}\right)J + (\alpha(GP))M}. \quad (3.14)$$

The  $\frac{GP}{GP_J}$  term or spreading gain is assumed to be approximately equal to one for wideband interference [PZB95]. The experiments that follow do not include any “jamming” sources, but the calculations are included in the model for completeness. Using the previous assumption, rearranging and generalizing (3.14) gives

$$SIR = \frac{S_i}{\frac{1}{GP} \left( N + \sum_{p=1}^r J_p \right) + \sum_{q=1}^t \alpha_q M_q} \quad (3.15)$$

where  $S_i$  is the transmitted power of the SOI,  $r$  is the number of jammers and  $t$  is the number of MAIs. It is clear that  $GP$  is the key factor in reducing interference caused by ambient noise and jammer interference, while the cross-correlation value,  $\alpha$ , is key in reducing the effect of MAI on the SNR of the signal of interest. The second experiment described below validates the use of the cross-correlation value in the multiple access portion of this equation.

*3.12.1.4 Model Setup for Experiment.* The configuration for the modeled system is shown in Figure 3.4. The MAI is set up as three separate stations. The 6 dB station is turned on first since it is the lowest power setting. At this point, the total MAI equals the 6 dB level in Table 3.1. The MAI power is increased to the 5 dB level by “turning on” the 5 dB transmitter. The transmitter’s power is set so that the addition of the transmission results in the 5 dB MAI level. Finally, the 4 dB station is “turned on” for the last MAI power setting. This was done to further verify that the model properly accounted for multiple transmitters.

*3.12.2 CDMA LAN Test Bed.* This section describes the test bed system characteristics and the setup of the test bed.

*3.12.2.1 Test Bed Characteristics.* The DS/CDMA development board test bed configuration includes the following characteristics:

- The transmitters and receiver tap a single bus channel,
- Noise on the channel includes all sources,
- Pass band transmission,
- Imperfect power control and
- Imperfect synchronization.

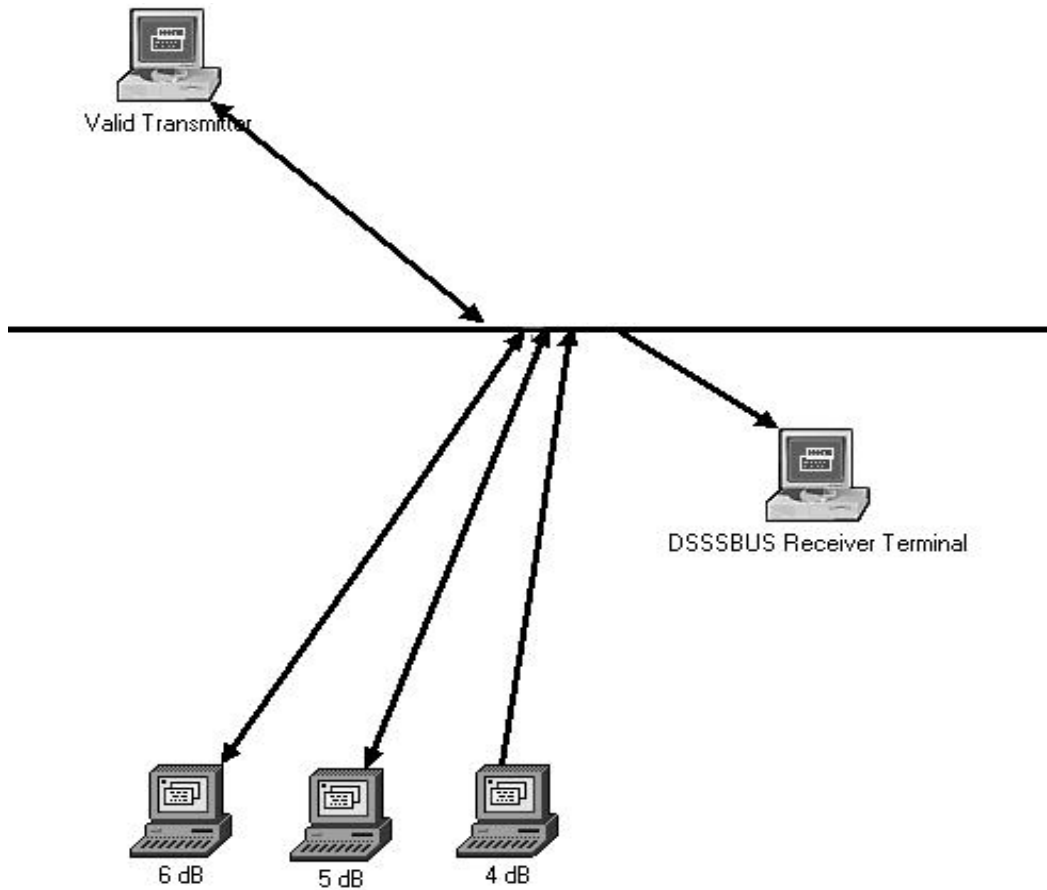


Figure 3.4 OPNET model configuration for experiment 2.

The method of analyzing data from the test bed alleviates non-uniformity of transmission sizes caused by imperfect synchronization. The method is discussed below in experiments.

*3.12.2.2 Test Bed Setup.* The Waveplex board is setup in loop back mode so it receives the data it transmits. The Waveplex SS board transmission is the SOI. The only other transmitting source in the setup is the interference source. It transmits its null data onto the bus with a spreading code that is in the same code family, but is not the PN sequence which the receiver is using to despread data. Both sources use 31-bit maximal length sequences. The SOI is spread with a

sequence created by shift register taps 5 and 2 while the interference uses taps 5,4,2, and 1. Figure 3.5 shows the DS/CDMA test bed hardware setup.

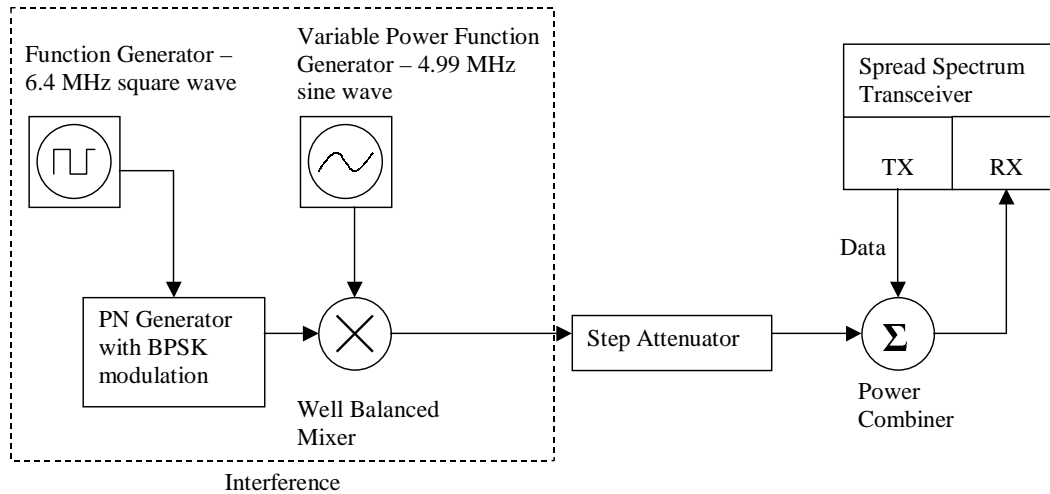


Figure 3.5 Hardware setup of DS/CDMA LAN test bed for experiment 2.

The interference source is created with the four components enclosed in the dashed box. The 31-bit maximal length sequence with taps 5,4,2,1 is constructed by the PN generator set to BPSK modulation. The generator's chipping rate is externally clocked by a square generator clocked at 6.4 MHz. The baseband SS signal is up-converted to 4.99 MHz via a Hewlett Packard function generator clocked at 4.99 MHz and a mixer. The HP 8645A agile function generator's power was set to -11.0 dB. The AMI SS board is setup to transmit a 4.99 MHz intermediate frequency (IF). The sine wave generator is capable of varying its signal power which could vary the resultant mixed signal. However, since a mixer is a non-linear device, this would create inaccurate output power levels. Thus, a step attenuator, which is a linear device, is used. The attenuated interference source is combined with the SOI from the Waveplex SS board via a voltage divider/combiner (also called a power splitter). The combiner is used in lieu of a coaxial T-junction because it provides better impedance matching. The combiner acts as the network bus in this setup. The combined signal is input into the Waveplex SS receiving unit. The parts mentioned above are described in detail in Appendix B.

*3.12.3 Experiments.* Two experiments are conducted to validate the OPNET DS/CDMA LAN model. The first experiment validates the link properties simulated in OPNET for the 10base-2 cable. The second experiment validates the MAI by comparing BER performance of the model and test bed.

*3.12.3.1 Experiment 1.* Experiment 1 consisted of first validating the coaxial loss model on the various lengths of coaxial cable with a cable analyzer and comparing the attenuation values to those observed in a simulation run of the modeled DS/CDMA LAN. Frequencies ranging from 2 to 45 MHz were tested on a cable analyzer at the three cable lengths. The attenuation was recorded for each setting. The recorded samples are compared to the coaxial loss model with a paired sample comparison test. Next, the test bed was configured to compare measured spread spectrum attenuations with the coaxial loss equation. The distance between the transmitter and receiver and the length of the cable are varied with values of approximately 50, 100 and 194 feet. The chipping rates, and therefore the transmitted bandwidth, are varied with values, 3.05 MHz, 5.81 MHz, 21.3 MHz.

A full factorial experiment is run with these two factors and their three levels. Two points of each setting are measured and analyzed. The peak voltage near center and the 2nd lobe peak voltage. The peak voltage “near” center is chosen since the center frequency actually has a null value. The peak voltage near center approximates the peak voltage of the signal. Attenuation measurements from the measured and simulated results are compared. The results of this experiment are presented in the next chapter.

*3.12.3.2 Experiment 2.* The second experiment validates the multiple access characteristics of the OPNET model. BER variations from the test bed implementation are measured on a single receiver when multiple transmitters are transmitting concurrently on the same bus. The multiple transmitters are simulated by varying power levels of a single DSSS interference source. These results are

compared with the variations of the identical metrics on a duplicate scenario in the OPNET model.

The factor used for this experiment is the amount of transmitted power from the DSSS interference source. The power is varied from the single source via a step attenuator that attenuates the power by 4, 5 and 6 dB.

Data is sent to the Waveplex SS board via a serial link to a PC, transmitted, received by the board, and then sent back to the PC via the same serial link for display on the terminal emulator. The data sent is compared to the received data in order to calculate the BER of the test bed. The BER is collected for each power level then a single factor analysis of variance (ANOVA) is performed. The ANOVA confirms whether the variation in measured BER is due to the levels of interference power.

The BER for the 4 dB attenuation level is used to empirically determine a cross-correlation value,  $\alpha$ , that produces an identical BER in the OPNET model. With the determined  $\alpha$ , BERs are simulated for the 5 and 6 dB attenuation levels. The simulated BERs are compared to the measured BER using a paired sample comparison.

*3.12.4 Experimental Error and Normalcy.* Variation due to experimental error was measured for experiment two with ANOVA. A residual quantile-quantile plot was made to verify that the errors are normally distributed. The residuals versus responses were plotted to verify a independence of errors from the levels.

*3.12.5 Verification and Validation.* Measurement validation is performed for the AMI SS board measurements by comparing measured values to published values. Simulation validation is performed by comparing calculated BER with the resulting bit errors per valid packet in the simulation. These results are presented

in Chapter IV. Model verification is accomplished by analyzing packet traces and is presented in Appendix C.

### *3.13 Summary*

This chapter presented the goals of this research as well as the methodology in which this research follows in order to achieve the goals. It presented the relevant parameters of the systems under test and the factors that are varied to analyze the system behaviors and validate the DS/CDMA LAN OPNET model. It presented the experimental designs this research implements and analyzes. A detailed description of the DS/CDMA LAN test bed was also provided. Chapter IV shall present the results and analysis of the experiments described in this chapter.



## IV. Results and Analysis

This chapter presents the results from this research. Validation of the measurement methods is discussed. Modified DS/CDMA bus simulation model validation is conducted and analyzed. Model verification is presented in Appendix C. The results from the two experiments described in the previous chapter are also presented and analyzed. Hardware used to gather data is described in Appendix B.

### 4.1 Validation of Measurements

To validate the spectrum analyzer measurements of the transceiver output, measurements are compared to the outputs specified in the board operating manual. There are three transceiver settings used in this research. Each setting has parameters that produce output center intermediate frequencies (IF) and bandwidth.

*4.1.1 Waveplex Board Operation.* Each setting has parameters affecting various clocks within the system that ultimately affect the resultant center frequency and bandwidth. These clocks are calculated by register settings of the system demodulator and spread spectrum processor integrated chip (IC). Each setting's demodulator IF center frequency,  $F_{IF}$ , and bandwidth settings are dependent on each of the parameters in Table 4.1.

Table 4.1 Spread spectrum transceiver register settings and clock frequencies.

	chip_rate	$F_{Ref}$ (MHz)	Div_ 25_50	Div_ 1_16	$F_{VCO}$ (MHz)	$F_{clk}$ (MHz)	$F_{offset}$
Setting 0	20	2	25	4	50	25	26214
Setting 1	10	2	25	2	50	50	13107
Setting 6	2	2	25	4	50	25	26214

This table shows the settings and their values that need to be programmed into the transceiver's register and the demodulator. The chip\_rate used to calculate the transmitted chipping rate,  $R_c$ , where,

$$R_c = \frac{64\text{MHz}}{\text{chip\_rate} + 1}. \quad (4.1)$$

The reference frequency,  $F_{ref}$ , is constant for each setting and is defined by the demodulator reference crystal. `Div_1_16` and `Div_25_50` are register values that are used to calculate both  $F_{VCO}$ , voltage controlled oscillation frequency, and  $F_{Clk}$ , the demodulator internal clock frequency.  $F_{VCO}$  is

$$F_{VCO} = F_{REF} \cdot \text{Div\_25\_50}. \quad (4.2)$$

$F_{Clk}$  also helps determine the data rate, which is not considered here.  $F_{Clk}$  is based on  $F_{VCO}$

$$F_{Clk} = F_{VCO}/\text{Div\_1\_16}. \quad (4.3)$$

The Waveplex development board contains a 10 MHz crystal that always results in a 5 MHz center IF frequency,  $F_{IF}$ . The  $F_{offset}$  register value must be set such that

$$F_{IF} = 5 \text{ MHz} = F_{offset} \cdot F_{clk}/2^{17}. \quad (4.4)$$

This allows proper operation for other aspects of the system such as demodulation [AMI61].

The IF null-to-null bandwidth,  $(BW_{IF})_{N-N}$ , is the positive frequency components of the transmitted spectrum that exist between the first null on either side of the  $F_{IF}$  [Sk188]. It is calculated as

$$(BW_{IF})_{N-N} = \begin{cases} 2 \cdot R_c, & R_c \leq F_{IF} \\ F_{IF} + R_c, & R_c > F_{IF} \end{cases} \quad (4.5)$$

Each setting's chip rate, IF center frequency and null-to-null bandwidth from the equations above are shown below in Table 4.2.

Table 4.2 Settings' theoretical BW,  $F_{IF}$  and chip rate.

	chip rate (MHz)	$F_{center}$ (MHz)	Bandwidth (MHz)
Setting 0	3.05	4.999	6.1
Setting 1	5.82	4.999	10.819
Setting 6	21.3	4.999	26.299

4.1.2 *Measured operational characteristics.* The power spectral density (PSD) of each setting are shown in Figures 4.1, 4.2, and 4.3.

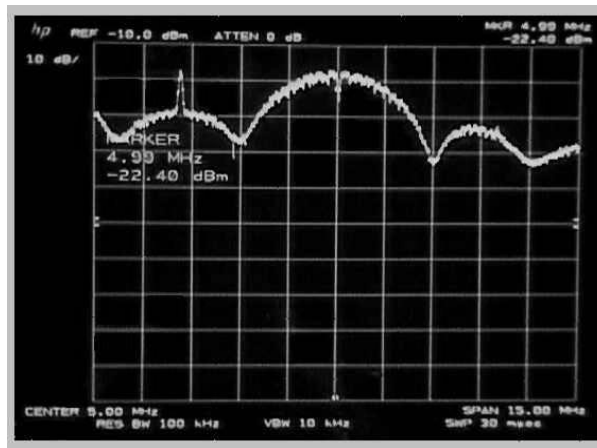


Figure 4.1 Setting 0 Power Spectral Density.

Figure 4.1 displays the Waveplex board default setting 0 logarithmic PSD. Decibels with reference to 1 milliwatt (dBm) versus Hertz is displayed. The display is centered on 5 MHz. Each horizontal division represents approximately 1.5 MHz. Each vertical division represents 10 dB difference with the top or reference level equaling -10dB. As Figure 4.1 shows, the  $F_{IF}$  is set at 5 MHz, which is evident by a drop of about 4.92 dBm at the center frequency. Using (4.5) and the approximate nulls at 2 and 8 MHz, the chipping rate was found to be 3 MHz.

Figure 4.2 shows the Waveplex board default setting 1 logarithmic PSD. The display parameters are listed in Table 4.3. The characteristic drop in voltage occurs

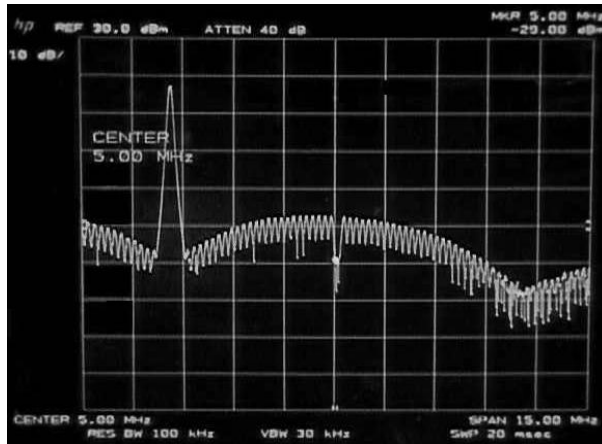


Figure 4.2 Setting 1 Power Spectral Density.

at approximately 5 MHz while the positive null exists at approximately 10.54 MHz yielding an actual chip rate of approximately 5.54 MHz.

Table 4.3 Display Settings for Figure 4.2

Center Frequency	5 MHz
Frequency Span	15 MHz
Hz/division	1.5 MHz
Reference level (Top)	30 dBm
dB/division	10 dBm

Figure 4.3 shows the Waveplex board default setting 6 logarithmic PSD. The display parameters are summarized in Table 4.4. Figure 4.3 only displays 15 MHz of setting 6 bandwidth to present the null at the center frequency 5 MHz. Figure 4.4 shows setting 6 in the linear scale, Volts per Hertz, and displays the entire bandwidth. Table 4.5 summarizes the display settings.

Table 4.4 Display settings for Figure 4.3.

Center Frequency	5 MHz
Frequency Span	15 MHz
Hz/division	1.5 MHz
Reference level (Top)	-10 dBm
dB/division	10 dBm

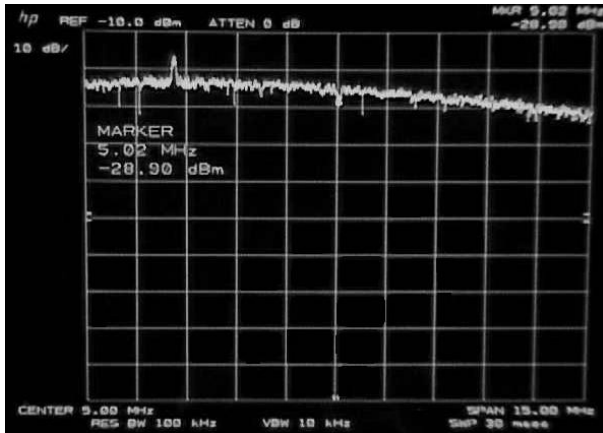


Figure 4.3 Setting 6 Power Spectral Density (zoomed to center).

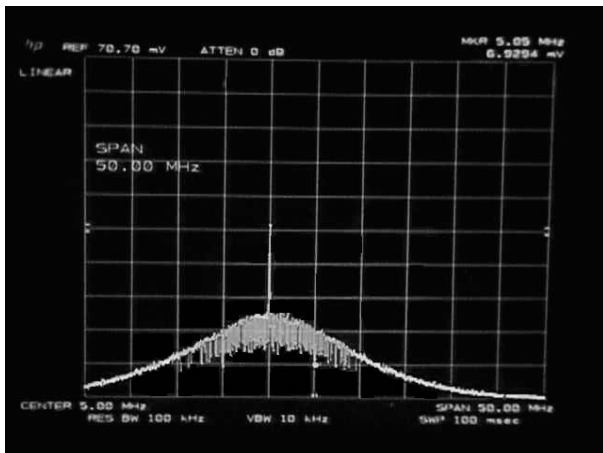


Figure 4.4 Setting 6 frequency spectrum (full bandwidth).

Table 4.5 Display settings for Figure 4.4.

Center Frequency	5 MHz
Frequency Span	50 MHz
Hz/division	5 MHz
Reference level (Bottom)	0 Volts
V/division	7.07 mV

Setting 6 in Figure 4.4 shows a signal with a first null at approximately 25 MHz. There was also secondary lobe power in higher frequencies such as 42 MHz not shown in figure. Since the signal is spread over 30 MHz with the same available power as settings 0 and 1, exact measurement of the null-to-null bandwidth is problematic.

The peak voltage of setting 6 was also difficult to measure since the DC component of the measuring equipment was so relatively close to the center of the spread signal. The peak voltage actually occurred very close to 0 Hz. Each setting displayed similar measurements to their theoretical values. In settings 0 and 1 it was apparent that the bandwidth and chip rate were slightly smaller than theoretical. The chip rates were smaller by 50 kHz and 320 kHz, respectively. A peculiar characteristic of the board that can be seen in each PSD is that the power seemed to be slightly higher to the left of the center frequency. Nevertheless, the similarity of measurements is sufficiently close to theoretical values.

*4.1.3 3dB Bandwidth Reduction.* The 3dB bandwidth for setting 6 reduced as the cable lengths were increased. The 3dB power bandwidth, also called the half-power bandwidth, is defined as the range of frequencies over which the signal power does not drop below 3dB the peak response at center frequency [Skl88]. As Figure 4.5 shows, the 3dB bandwidth dropped as cable length increased. Further analysis of this effect showed that the spectrum analyzer could not accurately measure this setting.

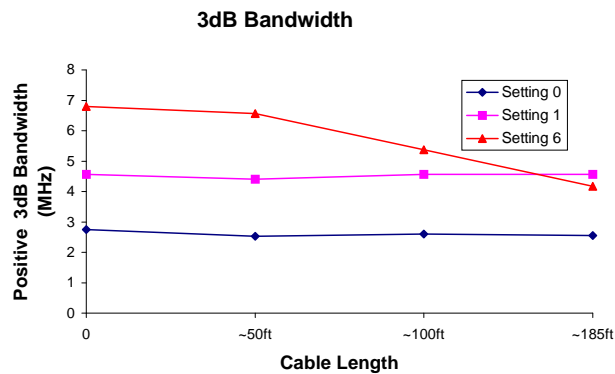


Figure 4.5 3dB Bandwidth measurements for Waveplex Board settings.

Detailed analysis is presented in Appendix D. It shows that the measurements for setting 6 were not valid. Therefore, the setting is omitted from further analysis.

## 4.2 DS/CDMA OPNET Model Validation

Validation of the DS/CDMA bus model was performed on a test configuration of the DS/CDMA system. A single transmitter and single receiver were connected in a bus configuration to show that the calculations within the pipeline stages truly reflected known behavior of such systems. Validation ensured the calculated bit error rate curve was consistent with the BPSK coherent signaling bit error rate [Sk188]. Furthermore, it ensured that the allocated BER to received packets is statistically equal to the calculated bit error rate.

Figure 4.6(a) shows the calculated BER of the model as the SNR is increased. Figure 4.6(b) shows the theoretical BPSK coherent signalling BER curve.

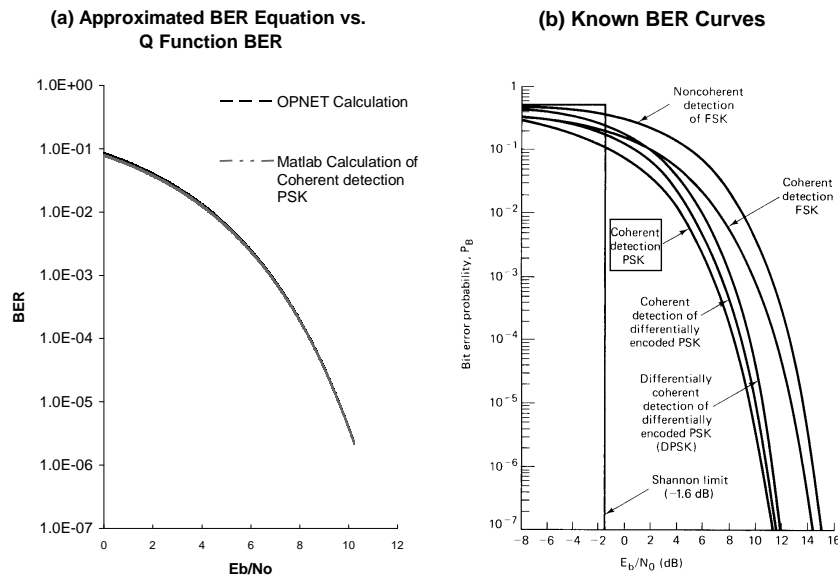


Figure 4.6 BER curve comparison (a)OPNET calculated BER from SNR and BER curve from actual Q function (b)BER curves with BPSK coherent signalling highlighted [Sk188].

The purpose of this comparison is to validate the conversion of SNR to  $E_b/N_0$  within the OPNET pipeline stage for BER calculation. The OPNET calculated errors were plotted against the theoretical BER given by (3.1) calculated by Matlab. Figure 4.6 shows that the OPNET BER calculations closely follow the theoretical BER. The results of the comparison showed that the OPNET BER overestimated

the theoretical by at most 0.08%. Its prediction monotonically improved for higher SNRs — the difference dropped to less than 0.02%.

To validate that the model is assigning the correct number of bit errors to the received packets, the allocated BER per packet statistic is compared against the calculated BER for the appropriate SNR level. Figure 4.7 shows the results of the allocated BER per packet when the SNR is increased from -8 dB to 12 dB. It also shows the calculated BER curve.

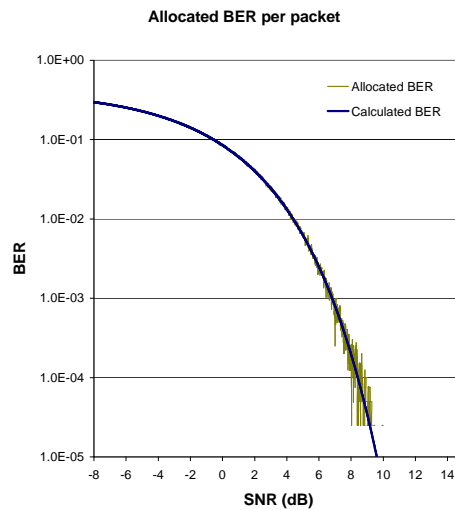


Figure 4.7 OPNET packet BER curve with calculated BER curve

It is important to note there are no simulated BER values equal to or less than the order of  $10^{-3}$  because the simulated packet sizes are 40,000 bits (5000 bytes) long and the model allocates zero bit errors to that packet. The model sets the allocated BER on a packet per packet basis. As the calculated BER approaches negative infinity, the chance of bit errors in a 40,000 bit packet becomes less and less, therefore, the allocated BER is approximately zero for SNRs greater than 11 dB. As Figure 4.7 shows, the allocated BER and the calculated BER were shown to be statistically equal using a paired sample test with 90% confidence. The mean difference was  $2.59E-05$  and the standard deviation was  $2.2E-03$ . The validation of



model behavior shows that the receiver module behaves as a BPSK coherent signal receiver as described in [Sk188].

The results of validation conclude that DS/CDMA bus model behaves similar to the DS/CDMA model described in [Bon01]. They also show that the bus model accounts for the physical characteristics of the RG-58 coaxial cable.

### 4.3 Attenuation Experiment

This section presents the results from experiment 1. It presents the validation of the analytic attenuation model with cable analyzer measurements and then compares the model to actual SS attenuation.

*4.3.1 Validation of Analytic Attenuation Model.* The analytic attenuation model introduced in Chapter 2 and restated below in equation 4.6 is validated by a series of measurements using a MFJ cable/antenna analyzer [MFJ99]. The cable analyzer is capable of measuring the attenuation of signals at various frequencies. Cable loss measurements were taken from 2 - 45 MHz for each length of cable. The cable analyzer was not able to measure attenuations less than 0.28 dB at the 1.7 - 4 MHz level. Figures 4.8, 4.9, and 4.10 show the attenuations of 50, 100 and 194-foot cables, respectively at various frequencies.

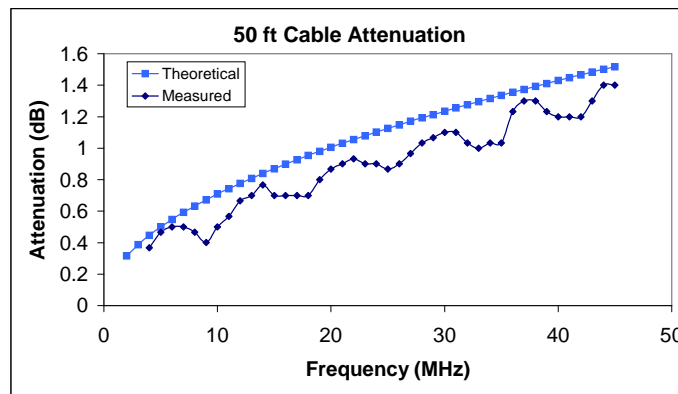


Figure 4.8 50 foot cable analyzer attenuation measurements and theoretical values.

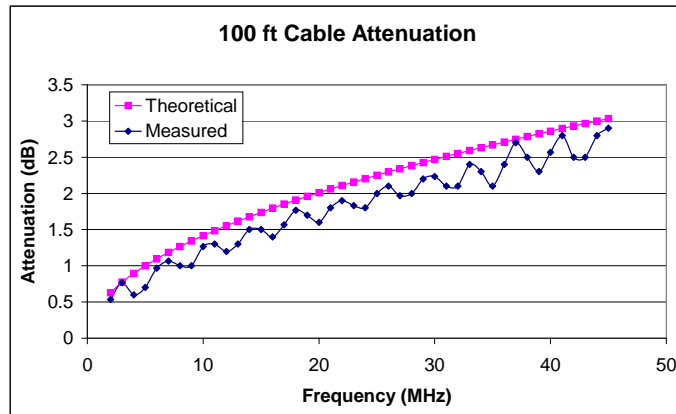


Figure 4.9 100 foot cable analyzer attenuation measurements and theoretical values.

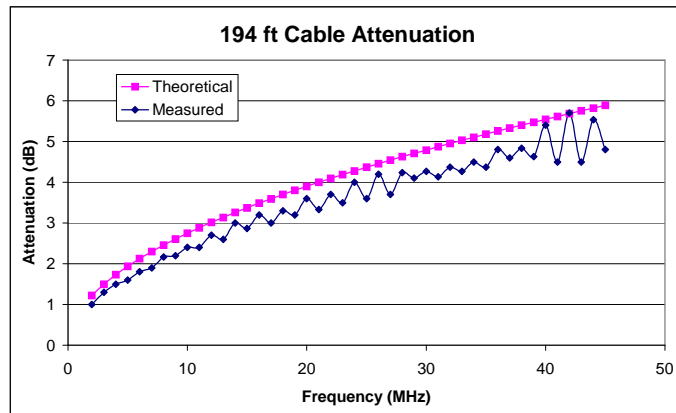


Figure 4.10 194 foot cable attenuation measurements and theoretical values.

The figures show that the analyzer cable attenuation readings are bounded from above by theoretical values. Figure 4.10 shows two measured data points that passed the theoretical upper bound. The random and periodic measured attenuation responses are caused by random and periodic impedance variations in the coaxial cable [Tim01].

A paired sample test was conducted. The average difference between the measured and theoretical values was calculated for each cable length. Their 90% confidence intervals are presented in Table 4.6.

Table 4.6 C.I.s of difference between MFJ measured and theoretical attenuations.

Cable Length (feet)	Theoretic and Measured Difference (in dB)	
	Lower 90% C.I. bound	Upper 90% C.I. bound
50	0.15	0.19
100	0.25	0.32
194	0.27	0.39
All measurements	0.24	0.27

These data suggest that the analytic model for RG-58 coaxial cable [Tim01],

$$A_{RG58} = 0.444 \cdot \sqrt{F_{MHz}} + 0.00126 \cdot F_{MHz}, \quad (4.6)$$

overestimates the attenuation,  $A_{RG58}$ , for the set of cables used in this experiment. Equation 4.6 overestimates the actual measurements by an average of 0.28 dB when all measurements are considered. This bias can be attributed to manufacturing of this particular cable. The measured responses follow the theoretic curve, so the coaxial loss model is a reasonable approximation for cable attenuation. The data, summarized in Table 4.6, shows that the variance of the measurements increases with cable length. Figures 4.8, 4.9, and 4.10 display an increase in response variance with frequency. This is attributed to normal impedance variations.

*4.3.2 Spread Spectrum Attenuation.* The second goal of the first experiment described in Chapter 3 is to observe the attenuation of a spread spectrum signal over varied lengths of RG-58 coaxial cable. Two settings of the AMI Waveplex developmental spread spectrum transceiver are used to observe attenuation over the cable. The settings are described in the beginning of this chapter (c.f., Table 4.2). The signals were measured using a Hewlett Packard 8568B spectrum analyzer. Attenuation measurements discussed below reflect the difference in peak power levels (in dBm) from a reference configuration consisting of a transmitter and spectrum analyzer connected by a two foot RG-58 coaxial cable to approximate zero attenuation. Measurements from both Waveplex board settings including center lobe and second

lobe peaks are combined and analyzed. The attenuation measurements in dB over each cable are displayed and analyzed below. Attenuation measurements from the cable analyzer and theoretical attenuation values are also displayed for comparison. Figure 4.11 shows attenuation measurements for the 50-foot cable.

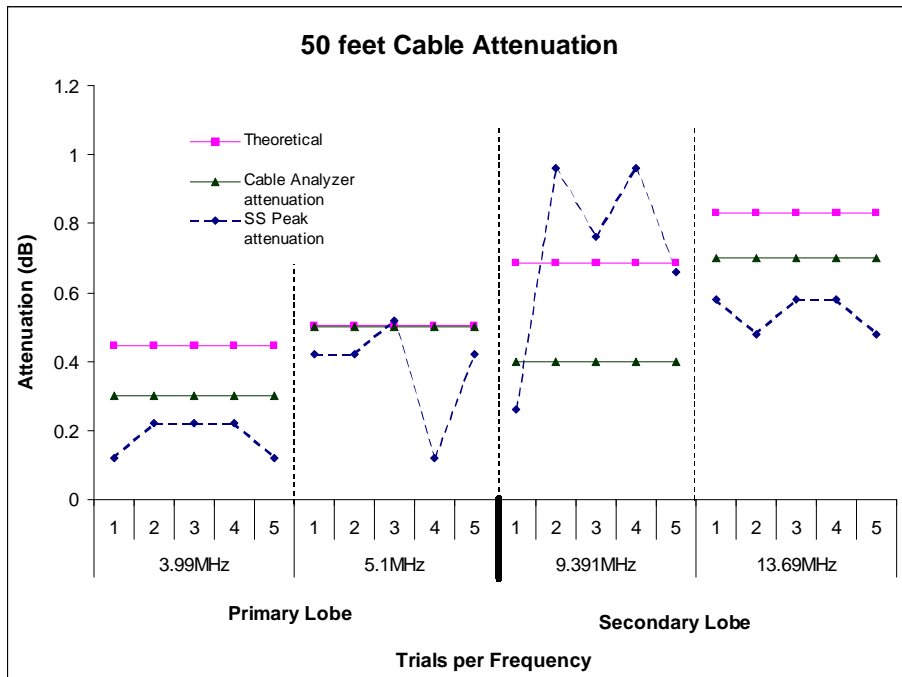


Figure 4.11 Comparison of primary and secondary peak frequency 50-foot attenuations.

The cable analyzer and SS measurements were measured in 5 independent trials for each frequency. The theoretical value is repeated for comparison. At 50 feet, the SS peak attenuation came within 0.08 dB of the theoretical value. It statistically equaled the measured attenuation from the cable analyzer. The average differences were 0.16 and 0.02 dB, respectively. Figure 4.11 shows the three types of measurement, analytic, cable analyzer and SS peak and second lobe peak power responses for comparison. Figure 4.12 shows the attenuations at 100 feet.

Measurements on the 100-foot cable display a divergence of the SS peak response measurements from both the theoretical and the cable analyzer measurements. Paired sample tests show that for the 100-foot cable the average difference

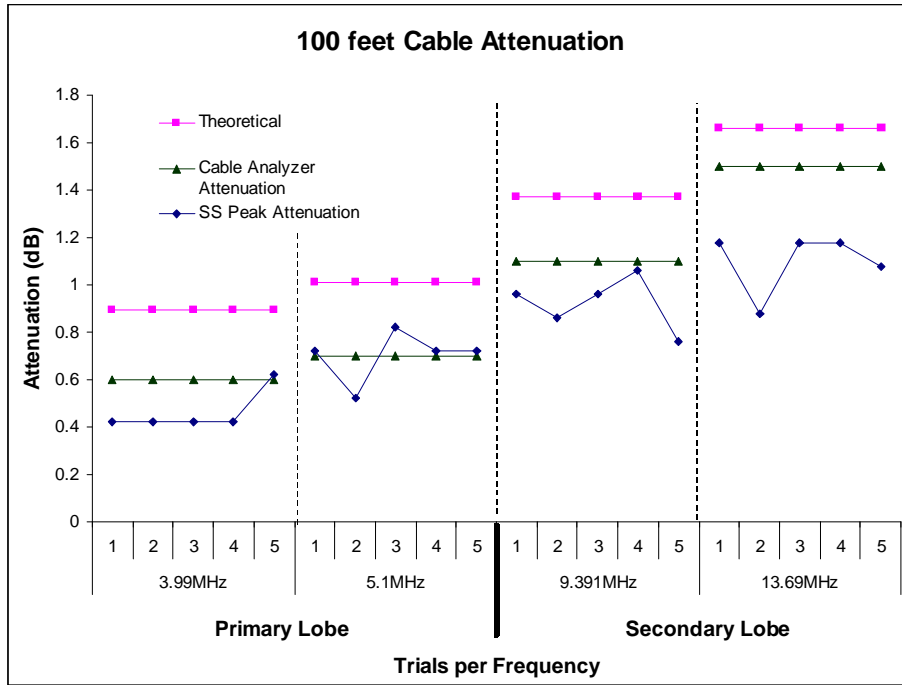


Figure 4.12 Comparison of primary and secondary peak frequency 100-foot attenuations.

between the SS and theoretical attenuation is 0.44 dB and the difference between the SS and cable analyzer measurements is 0.18 dB. Figure 4.13 displays the attenuation responses for the 194-foot cable.

As Figure 4.13 shows, the coaxial loss (4.6) overestimates the SS attenuation. The average difference between the predicted and SS attenuation is increased to 0.64 dB. The average difference between the cable analyzer measurements and the SS spectrum analyzer measurements increased to 0.345 dB. The results were unexpected. The cable analyzer and SS attenuations were expected to be equal throughout. They were statistically equal for the 50-foot measurements, but their difference grew with cable length. The differences are a fraction of a dB and could be caused by losses in the connectors used for the hardware measurements. The cable analyzer needed two separate connection converters to measure the cable loss, while the SS measurements did not. The connectors are described in Appendix B.2. Figure 4.14

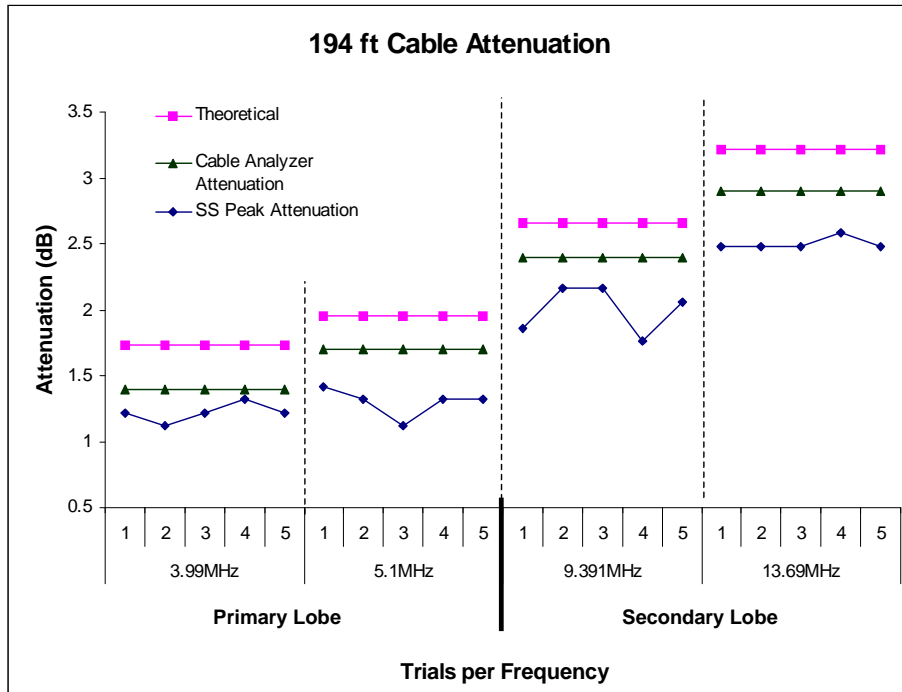


Figure 4.13 Comparison of primary and secondary peak frequency 194-foot attenuations.

summarizes the 90% confidence intervals of each paired sample difference described above. Table 4.7 displays the data used in Figure 4.14.

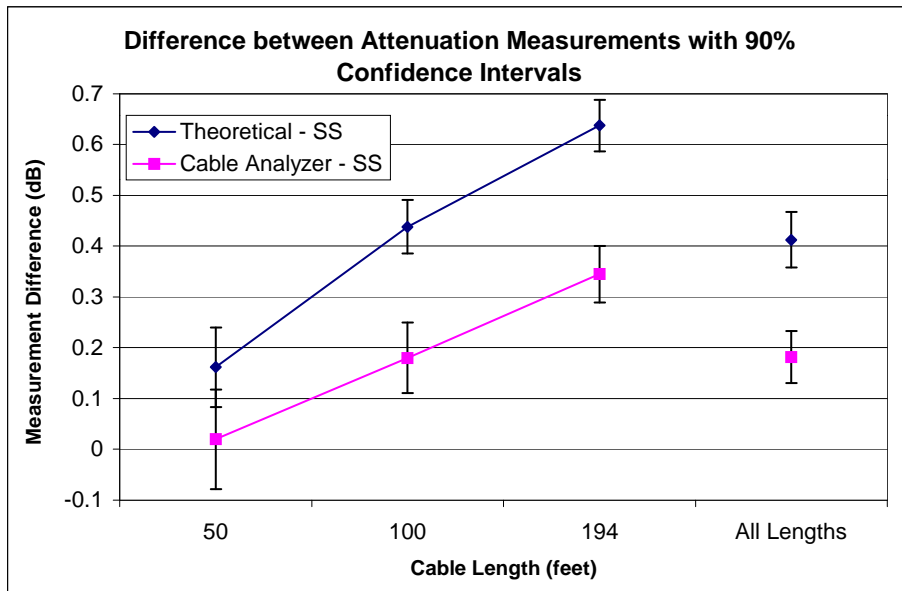


Figure 4.14 Summary of experiment 1 analysis.

Table 4.7 Summary of data for Figure 4.14

<b>Difference between Theoretical and SS Attenuation</b>			
<b>Cable Length</b>	<b>Lower 90 %C.I. Bound</b>	<b>Mean Difference</b>	<b>Upper 90% C.I.Bound</b>
50 ft	.083	.162	.240
100 ft	.385	.438	.492
194 ft	.587	.638	.689
Total	.358	.413	.467
<b>Difference between Cable Analyzer and SS Attenuation</b>			
<b>Cable Length</b>	<b>Lower 90 %C.I. Bound</b>	<b>Mean Difference</b>	<b>Upper 90% C.I.Bound</b>
50 ft	-0.078	.02	.118
100 ft	0.111	0.18	0.249
194 ft	0.290	0.345	0.400
Total	0.131	0.182	0.233

Each curve displayed in Figures 4.11, 4.12 and 4.13 follows the same trend. Table 4.7 and Figure 4.14 also present the total difference for all cable lengths between the theoretical and SS attenuations and the cable analyzer and SS measured attenuations. The differences are a small percentage of the total attenuation, so the model does describe the actual attenuation curve, and offers an upper bound worst case for attenuation modeling of a 10Base2 coaxial cable. As described in section 4.3.1 and shown in section A.1.2, a small bias could be applied to the coax loss (4.6) that would help better describe the measurements.

#### 4.4 Bit Error Rate Comparison

The second experiment compares measured BER rates of the spread spectrum board with varied levels of interference and the DS/CDMA bus model with similar interference. Results and analysis of this experiment are discussed below. First, the BER measurements of the test bed are discussed in detail. Then, the test bed and the OPNET model BER are compared.

*4.4.1 Measured Bit Error Rates.* This section presents the results from the test bed BER measurements.

4.4.1.1 *Test Bed Setup.* The hardware portion of this experiment uses the test bed setup as described in Chapter 3. Implementation of the setup is further described here. A spread spectrum interference source was simulated as a MAI source by matching its code length, chipping rate, consequently the  $BW_{N-N}$ , and  $F_{IF}$ , with that of the Waveplex transmission. The matching was accomplished empirically by measuring the produced MAI signal and adjusting accordingly. The final non-attenuated output is displayed in Figure 4.15.

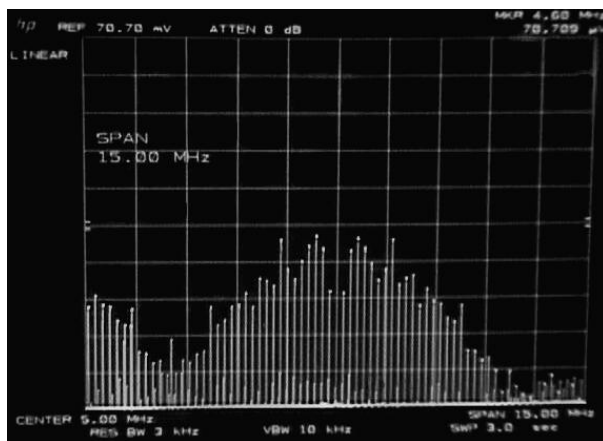


Figure 4.15 Summary of experiment 1 analysis.

The display parameters are summarized in Table 4.8. The produced MAI

Table 4.8 Display settings for Figure 4.15

Center Frequency	5 MHz
Frequency Span	15 MHz
Hz/division	1.5 MHz
Reference level (Bottom)	0 mV
V/division	7.07 mV

signal displayed a center frequency of 4.99 MHz and a  $BW_{N-N}$  of approximately 10.54 MHz. Theoretically, a 5.54 MHz sine wave should have been used to clock the SS word generator, however that setting produced a final  $BW_{N-N}$  that was less than the needed 10.54 MHz. The Tektronix sine-wave generator's frequency was incremented until the  $BW_{N-N}$  of the resulting signal and Waveplex SS board output



matched. This allowed enough reception stability at the 4dB attenuation to transmit and receive the entire transmitted file. Although the measurements were equal, the exact nulls could not be determined and there was inevitable non-synchronization in the PN clocks of the two systems. The non-synchronization caused a drift in the M-sequences so the correlation function of the sequences constantly changed.

*4.4.1.2 Challenges.* A transmitted file size was determined that would not overwhelm the Waveplex SS board first-in first-out transmit buffer and cause bits to be lost. The file size was 16,392 bits not including stop bits. The received file sizes were combined into larger blocks of bits that were between 100,737 and 118,737 bits long. These larger blocks are called trials in the analysis below. This was done to for two reasons. First, since each file transmission occurred with varying cross correlation functions it was assumed that larger blocks of received data would represent reception with an expected value of all the possible cross correlation functions. Second, due to numerous instances of lost synchronization in the middle of a file transmission, there were many different sizes of received files. Grouping the files into approximately equal sized blocks would allow the percentage of bit errors per block to have a more consistent meaning than bit errors per file when variance is analyzed.

BER measurement was somewhat subjective. The 4dB MAI attenuation level resulted in low SIR levels at the Waveplex SS receiver. Thus, the receiver lost synchronization quite frequently. Occasionally this occurred in the middle of a file transmission producing these outcomes:

1. The reception would end cleanly and just stop transmitting bits as if the transmitter was shut off;
2. A very high BER, on the order of  $10^{-2}$  was observed just before end of reception;
3. Erroneous data was received — unrelated bytes were deciphered by the receiver.

Other occurrences included added bytes and blocks of lost bytes. Different criteria were used in measuring bit error rates and yielded different results. One criterion was chosen for detailed analysis. The results found using other criteria are listed in Appendix A. This criterion was believed to be the most sound: a bit error was counted only if, in stable operation, an ASCII character was transformed to another printable or non-printable character. If a discrepancy was present when comparing the sent file to the received file, the byte was translated to its ASCII 8 bit equivalent, then compared bit by bit.

4.4.2 ANOVA. Using the criterion above, the BER was measured for each trial and a single factor ANOVA with unequal sample sizes was performed. Figure 4.16 shows the measured BER for each trial.

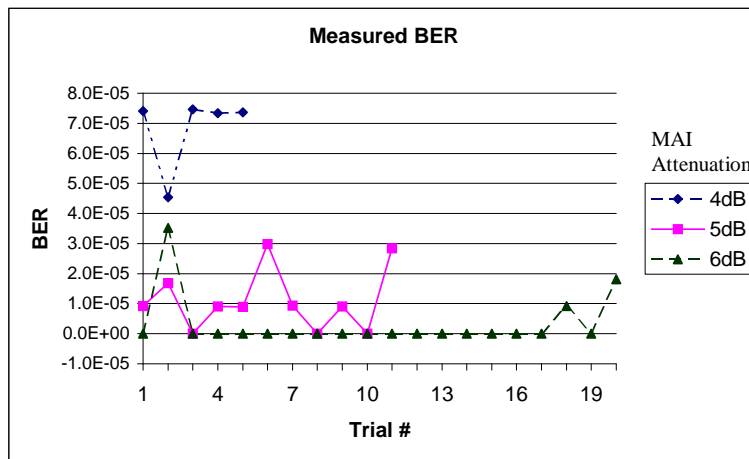


Figure 4.16 Measured BER of test bed per trial.

The varied number of samples is due to the level of difficulty in retaining synchronization during the file transmissions with higher MAI. The amount of data was believed to be sufficient in the higher powered MAI cases since the occurrence of bit errors was more frequent. Therefore, adequate proportions could be found for each trial size. The rank order of each BER was as expected. There were a few occurrences where the 6 dB setting shows higher BER than the 5 dB setting, but this is acceptable since the trials are a tool only for analyzing variance not overall

BER, which is presented below. Expanding the analysis window to remedy this would make it difficult to analyze the variance of the 4 dB BER results. The graph shows the 4 dB MAI power level to have the highest BER as was expected. Table 4.9 displays the ANOVA results for the responses in Figure 4.16.

Table 4.9 Analysis of variance of measured bit error rates

Source of Variation	Sum of Squares	Percentage of variation	Degrees of Freedom	Mean Square	F-Computed	P-value	F crit
MAI power levels	1.72E-08	0.84	2	8.58E-09	89.18	4.93E-14	2.47
Error	3.18E-09	0.16	33	9.62E-11			
Total	2.03E-08		35				

The results of the ANOVA test show that 84% of the variation is explained by the varied interference levels, while the rest is attributed to experimental error. A large part of the error can be explained by the subjectivity of measurements and the drift of the non-synchronous PN clocks. The F value for the ANOVA, shown in Table 4.9 is much larger than the critical F-value. Therefore, the variation of the interference level is significant with 90% confidence.

*4.4.2.1 Overall BER.* The overall BER of the system for each MAI level is calculated by taking the weighted mean of the BERs for each received file. In other words, for each power level, divide the total number of bit errors by the total number of transmitted bits over all the transmitted files. This also describes the proportion of bits with errors to the total bits sent. Thus, a confidence interval for proportions statistic can be used to summarize the results. Since the confidence interval for proportions uses the normal approximation for the binomial distribution the condition,  $np \geq 5$ , where  $n$  is the total number of trials and  $p$  is the proportion of errors, should be satisfied for each level [MiA95]. Table 4.10 displays the total results from the BER measurements, and the value  $np$  for each level. The sample proportion,  $p$ , is the overall BER for each level. The 90% confidence interval of each level's proportion is displayed in Table 4.11.

Table 4.10 Summary of Overall BERs for each MAI level.

Level	Bit Errors	Total Bits Sent, $n$	Sample Proportion, $p$	$n \cdot p$
4 dB	37	542,961	6.81E-05	36.98
5 dB	13	1,210,734	1.07E-05	13
6 dB	7	2,233,152	3.35E-06	7

Table 4.11 BER proportion 90% C.I.s

Level	Bounds
4 dB	(4.97E-05, 8.66E-05)
5 dB	(5.84E-06, 1.56E-05)
6 dB	(1.19E-06, 5.08E-06)

#### 4.5 OPNET and Test Bed BER comparison

The overall BER from each level, presented above, were compared with OPNET BER. First the cross correlation value,  $\alpha$ , was found empirically by comparing the OPNET model set up with a 4 dB MAI into the receiving terminal, until the BERs matched. The  $\alpha$  value found was 0.07112, which is between  $\frac{1}{31}$  (0.032) and  $\frac{9}{31}$  (0.29), the absolute values of the limits for the cross correlation function of a 31 bit maximum length sequence [PZB95]. It also lies between the squares of these values which may be a more appropriate bound since  $\alpha$  scales a interference power while the cross correlation coefficient may scale a voltage since it can take on negative values. The squares of the values are 0.001 and 0.0841. Next, the OPNET and test bed BERs for the 4, 5 and 6 dB MAI levels were compared. Using a paired sample test, the mean difference confidence interval was (-4.47E-06, 8.36E-07) with 90% confidence. Since the confidence interval includes zero, the two systems are considered statistically equal. Table 4.12 shows the paired data samples of this experiment.

Table 4.12 Paired data samples for measured and simulated BER comparison.

MAI attenuation	Measured BER	Simulated BER
4dB	6.81E-05	6.81E-05
5dB	1.07E-05	7.93E-06
6dB	3.13E-06	4.93E-07

#### *4.6 Summary*

This chapter presented the validation of the DS/CDMA bus model and the validation of measurement technique and the attenuation analytical model. It also presents results of two experiments comparing a DS/CDMA test bed to a DS/CDMA OPNET model. The conclusions as a result of these experiments are presented in Chapter 5.

## *V. Conclusions and Recommendations*

This chapter summarizes this research. The goal is restated and evaluated against the efforts of this research. The results are summarized and conclusions are made. Recommendations for further work in this area are presented.

### *5.1 Research Goals*

The goal of this research was to simulate a bus implementation of a direct sequence code division multiple access local area network and validate its simulated measurements with a hardware DS/CDMA LAN test bed. The validation was based on bit-error-rate and attenuation measurements.

### *5.2 Results*

The DS/CDMA test bed validated the signal-to-interference and BER calculations of the simulated system. The results showed that the two systems were statistically equal in BER measurements. Also, a proposed model for approximating cable attenuation was presented and validated against the test bed. The results in this analysis showed that the analytic model overestimated the measured power attenuation by approximately 0.3 dB.

### *5.3 Conclusions*

This research presents a validated bus implementation of a DS/CDMA LAN. The validation effort concentrated on the attenuation in the bus medium and the calculation of the signal-to-noise ratio that is used to figure the bit-error-rate. The overestimation of measured attenuation by the analytic attenuation model presents a worst case for future analysis of effects of power dissipation. However, it remains close enough to the actual value to be a good approximation. The model could easily be biased to better describe the measured frequencies.

The bit-error-rate comparison showed that the SIR calculation within the simulated DS/CDMA LAN is sound. The experiments used a varying cross-correlation number between the multiple-access interference and the signal-of-interest caused by the inability to synchronize the PN generators of the two transmitters. Since the results showed equal BER measurements (simulated and actual) it is concluded that a single value of a cross-correlation coefficient,  $\alpha$ , can be used to estimate the SIR in a multi-user environment as shown in (3.15). The coefficient will most likely describe the expected value of the code family's range of cross-correlation numbers.

The validated coaxial cable loss equation used describes undesirable attenuations at higher frequencies, i.e., 9.384 dB per 100 feet at 400 MHz. As more users are added to the network, the PN sequences must be longer and the chipping rate and bandwidth increased, possibly surpassing 400 MHz. If an adequate power control mechanism is not devised, the near-far effect could prove to be the downfall of this technique. A power-control algorithm that handles multiple receivers and transmitters would be very complex. On the other hand, carefully chosen pseudo-noise codes, such as Gold codes, could provide a low enough cross-correlation coefficient to effectively negate the near-far problem.

By validating the DS/CDMA model, the results of this research reaffirm the results found in [Bon01]. They confirm the dramatic improvement in network delay and throughput a DS/CDMA LAN displayed over Ethernet. Therefore, the DS/CDMA medium access control technique could be the technique of choice.

#### *5.4 Implications and Impact*

This model provides a vehicle for simulating CDMA LANs for any type of medium. It provides a fundamental foundation for accurately modelling the seven layers of the OSI network model when considering a fully functional, independent network node. This ground breaking research substantiates the grandiose claims of previous work — the declaration of a viable network medium access protocol

that offers enormous gains in network performance. This technology will transform communications as we know it.

The model may incorporate the attenuation properties of any medium due to its nature of modularity. The 10Base-2 cabling characteristics modelled in this research offer an important impediment that might cripple the CDMA technique over this medium. The cable attenuation could prove to create a huge mess in power control within the LAN. Station after station could starve from lack of SNR creating bit-error-rates too high to sustain functional communications.

If the near-far effect proves not to be a problem, the impact of this technology on the Air Force and entire Department of Defense alike will be far reaching. By simply switching a network interface card, communications within organizations will be significantly enhanced. Shared applications within organizations such as entire databases could be accessed without the frustrating wait time. Productivity of organizations relying on network shared data would greatly increase. Telecommunications would also be revolutionized. The increase in throughput and approximate elimination of delay would enable voice and video over the internet to be standard; the Air Force could do away with costly video conferencing rooms. All of these benefits could be attainable with minimal cost since no cabling infrastructure needs replacing.

### *5.5 Recommendations for Further Work*

The DS/CDMA - Carrier Sense Multiple Access with collision detection performance analysis conducted by [Bon01] assumed perfect power control and thus, ignored attenuation. With the bus implementation of DS/CDMA offered by this research, a new performance analysis could be conducted including cable attenuation and excluding power control. The new runs could again be compared with an Ethernet LAN as before to measure the effects of the near-far problem. If base-



band signalling is used, a representative frequency for the band would need to be determined in order to approximate power loss over the cable.

Another venue of research is to revisit capacity analysis for such a network. Tables of code lengths versus supported capacity could be constructed. Tables scaled by desired bit-error-rate performance would allow network designers to look-up an adequate capacity-performance combination to use for a given network.

This research mentions comparisons of asynchronous CDMA with Synchronous CDMA for a fibre optic CDMA LAN. In that case, S/CDMA allows higher capacities of simultaneous users. Further research could be accomplished in this area and a comparison made for a 10Base-2 CDMA LAN to improve user capacity or perhaps guarantee the lowest cross-correlation between codes to decrease effects of the near-far problem.

There remains a large amount of room for expansion of this DS/CDMA model. The model assumes that a receiver is receiving valid data from only one transmitter at all times. Expansion of the model towards a system similar to *Spreadnet* would allow more comprehensive performance analysis on a DS/CDMA LAN. Expansion could include implementing stations with multiple receivers that are able to receive from more than one transmitter at different times or at once. A new protocol should be developed to handle multiple incoming streams of data. It could dynamically assign PN codes to stations and length of codes to the network.

## 5.6 *Summary*

The research goals have been met. The simulation adheres to the real-world standard confirming validity of the model and the auspicious results that ensue. The attenuation investigation hints that the near-far effect will be a bump in the road, but further research could alleviate the problem in one way or another.

## Appendix A. Data Analysis

This section complements the results and analysis presented in Chapter IV. It presents the measurements taken for each experiment in tabular or graphical form as well as extraneous analysis. It also includes normality tests for the ANOVA performed for experiment 2 in Section 4.4.2.

### A.1 Experiment 1

This section presents the details of the waveplex board transmission measurements used in determining the attenuation of the SOI over varied cable length. Since setting 6 measurements were considered inaccurate, as discussed in Section 4.1.3 and appendix D, its data are not presented.

*A.1.1 Measurements.* The Waveplex SS board signal measurements for settings 0 and 1 are presented below in Table A.1 and Table A.2, respectively. The signal was separately measured for each cable length. All *levels* are given in dBm, while all *frequencies* are given in MHz.

Tables A.1 and A.2 show the average and standard deviation of various measurements from the SS signals. Average attenuations for each cable length are given for the peak frequency and the second lobe peak frequency. Attenuations were calculated against the average respective peak value on the *two-foot* cable. The confidence interval of the attenuation measurements is also given.

*A.1.2 Adjusted Coax Loss Equation.* It was mentioned in Chapter IV that a small bias applied to the coax loss equation would better predict attenuation for this set of cables. A pilot study was run to empirically find a new resistive loss constant that allowed a better prediction. The point of this study was to show that the curve produced by the given coaxial loss equation followed the trend of attenuation measurements. Figure A.1 shows the cable analyzer measurements for

Table A.1 Signal measurements with varied cable lengths for setting 0.

Waveplex Spread Spectrum Board Default Setting 0										
~2 foot cable	-3dB		Peak		-3dB		Null	2nd lobe peak		3dB BW (MHz)
	Level	Frequency	Level	Frequency	Level	Frequency	Frequency	Level	Frequency	
Average	-20.48	3.614	-17.48	5	-20.48	6.364	8.11	-31.94	9.376	2.75
Standard Deviation	0.204939	0.045607	0.204939	0	0.204939	0.0577062	0.0547723	0.1341641	0.0350714	
Average Attenuation and Confidence Intervals										
			0.38					0.72		
			90% C.I.					90% C.I.		
			0.2354111	0.5245889				0.4453308	0.9946692	
~50 foot cable	-3dB		Peak		-3dB		Null	2nd lobe peak		3dB BW (MHz)
	Level	Frequency	Level	Frequency	Level	Frequency	Frequency	Level	Frequency	
Average	-20.86	3.652	-17.86	5.084	-20.86	6.184	8.074	-32.66	9.432	2.532
Standard Deviation	0.1516575	0.0178885	0.1516575	0.0089443	0.1516575	0.0517687	0.1066771	0.2880972	0.0414729	
Average Attenuation and Confidence Intervals										
			0.70					0.92		
			90% C.I.					90% C.I.		
			0.5955613	0.8044387				0.8112967	1.0287033	
~100 foot cable	-3dB		Peak		-3dB		Null	2nd lobe peak		3dB BW (MHz)
	Level	Frequency	Level	Frequency	Level	Frequency	Frequency	Level	Frequency	
Average	-21.18	3.676	-18.18	5.14	-21.18	6.272	8.132	-32.86	9.3	2.596
Standard Deviation	0.1095445	0.0477493	0.1095445	0	0.1095445	0.0396232	0.0657267	0.1140175	0.2412468	
Average Attenuation and Confidence Intervals										
			0.70					0.92		
			90% C.I.					90% C.I.		
			0.5955613	0.8044387				0.8112967	1.0287033	
~194 foot cable	-3dB		Peak		-3dB		Null	2nd lobe peak		3dB BW (MHz)
	Level	Frequency	Level	Frequency	Level	Frequency	Frequency	Level	Frequency	
Average	-21.78	3.61	-18.78	5.076	-21.78	6.158	8.124	-33.94	9.456	2.548
Standard Deviation	0.1095445	0.0595819	0.1095445	0.0357771	0.1095445	0.0471169	0.0554977	0.181659	0.0482701	
Average Attenuation and Confidence Intervals										
			1.30					2.00		
			90% C.I.					90% C.I.		
			1.1955613	1.4044387				1.826808	2.173192	

Table A.2 Signal measurements with varied cable lengths for setting 1.

Waveplex Spread Spectrum Board Default Setting 1										
~2 foot cable	-3dB		Peak		-3dB		Null	2nd lobe peak		3dB BW (MHz)
	Level	Frequency	Level	Frequency	Level	Frequency	Frequency	Level	Frequency	
Average	-19.98	2.32	-16.98	4.51	-19.98	6.88	10.558	-31.22	13.97	4.56
Standard Deviation	0.0447214	0.1387444	0.0447214	0.0273861	0.0447214	0.1172604	0.0672309	0.083666	0.2043282	
Average Attenuation and Confidence Intervals										
			0.18					0.54		
			90% C.I.					90% C.I.		
			0.1277806	0.2322194				0.4877806	0.5922194	
~50 foot cable	-3dB		Peak		-3dB		Null	2nd lobe peak		3dB BW (MHz)
	Level	Frequency	Level	Frequency	Level	Frequency	Frequency	Level	Frequency	
Average	-20.16	2.44	-17.16	3.81	-20.16	6.84	10.558	-31.76	13.5	4.4
Standard Deviation	0.0547723	0.041833	0.0547723	0.0961769	0.0547723	0.1710263	0.0672309	0.0547723	0.3201562	
Average Attenuation and Confidence Intervals										
			0.46					1.10		
			90% C.I.					90% C.I.		
			0.3747261	0.5452739				0.9756931	1.2243069	
~100 foot cable	-3dB		Peak		-3dB		Null	2nd lobe peak		3dB BW (MHz)
	Level	Frequency	Level	Frequency	Level	Frequency	Frequency	Level	Frequency	
Average	-20.44	2.12	-17.44	3.8	-20.44	6.69	10.536	-32.32	13.72	4.57
Standard Deviation	0.0894427	0.0447214	0.0894427	0	0.0894427	0.065192	0.0680441	0.130384	0.2659887	
Average Attenuation and Confidence Intervals										
			0.46					1.10		
			90% C.I.					90% C.I.		
			0.3747261	0.5452739				0.9756931	1.2243069	
~194 foot cable	-3dB		Peak		-3dB		Null	2nd lobe peak		3dB BW (MHz)
	Level	Frequency	Level	Frequency	Level	Frequency	Frequency	Level	Frequency	
Average	-21.2	2.12	-18.2	3.84	-21.2	6.68	10.556	-33.72	13.57	4.56
Standard Deviation	0.0707107	0.0447214	0.0707107	0.0223607	0.0707107	0.0273861	0.0427785	0.0447214	0.5155095	
Average Attenuation and Confidence Intervals										
			1.22					2.5		
			90% C.I.					90% C.I.		
			1.1525851	1.2874149				2.4573631	2.5426369	

the 194 foot cable, as presented in Section 4.3.1, along with the new curve produced by reducing the resistive loss constant,  $k_1$ , to 0.39.

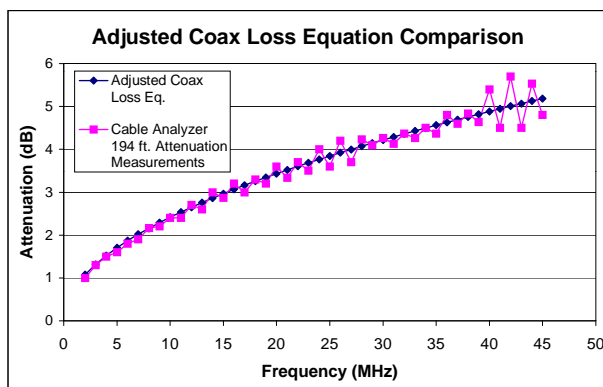


Figure A.1 Adjusted coax loss equation curve compared with 194-foot cable attenuations measured with cable analyzer.

Figure A.1 shows that the adjusted coax loss equation will predict attenuation up to 45 MHz. The limit is only due to research bounds. Visual analysis shows that the adjusted equation will probably predict the attenuation for even higher frequencies. A paired sample test was performed that yielded the mean difference 90% confidence interval of (-0.0863, 0.0374). Since the confidence interval includes zero, it can be said that the equation describes actual attenuation.

## A.2 Experiment 2

This section presents data on the second experiment namely, BER measurements from the Waveplex SS Board test bed setup. It presents different criteria that could be considered when measuring the BER rate in this experiment. BER measurements using these criteria are summarized. Finally, this section presents the normality tests to verify the correctness of the BER ANOVA.

*A.2.1 Measurements.* Figure A.2 graphically displays the detailed bit error measurements using the criteria discussed in Chapter IV. The three multiple access interference power levels are displayed along with their bit-error performance.

Recall that the 4 dB refers to the attenuation of a reference power signal, so 4 dB attenuation produces more interference than 6 dB.

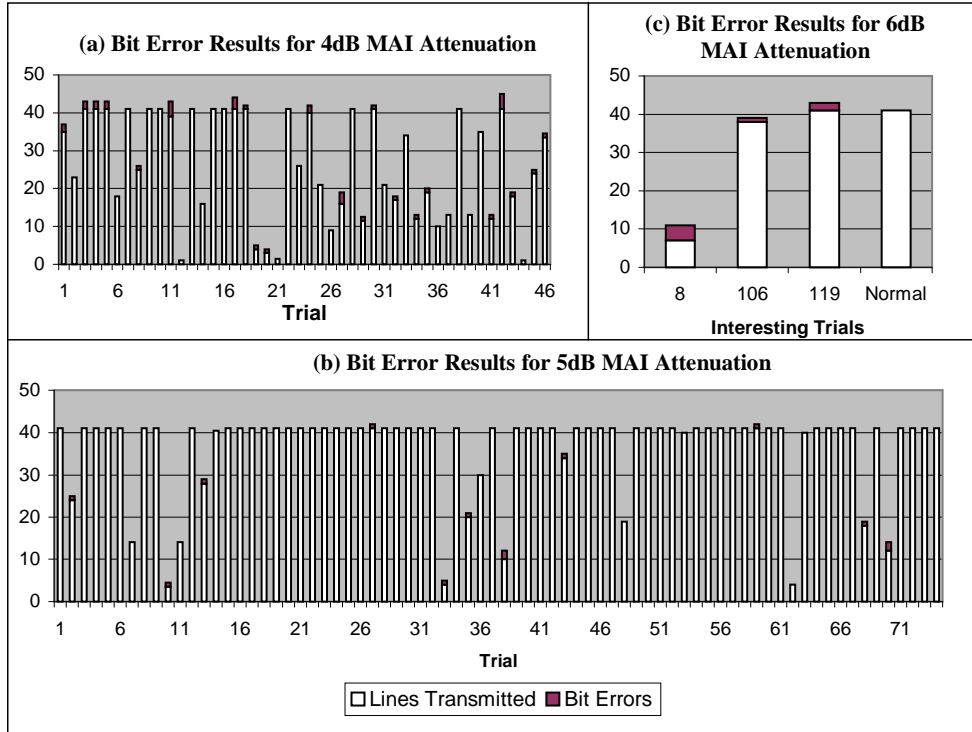


Figure A.2 Bit error measurements for three multiple access interference levels. (a) 4dB MAI level bit error results, (b) 5dB MAI level bit error results, (c) 6dB MAI bit error results.

The graphs in Figure A.2 display stacked statistics of the transmitted file size, in lines (where one line is 50 Bytes) and the number of bit errors for that file. The Y-axis interprets number of lines or number of bit errors. The 6 dB graph only displays files that actually had bit errors. Results from a non-error, *normal*, file are displayed for comparison; there were 122 files sent with 6dB level.

*A.2.2 BER Results with Varied Criteria.* As discussed in Section 4.4.1.2, there were many ways to judge the received bit errors in efforts to get the most accurate reading. Different criteria were created to observe actual bit errors. The reasons for these criteria are discussed in the fore-mentioned section. Different sizes of

the received data were recorded and different ways of tabulating errors were also used. The three sizes of total data referenced were transmitted data with and without stop bits and transmitted data with missing characters subtracted (without stop bits). Recall from 4.4.1.2 that some bytes were missing between normally transmitted data while at other times erroneous bytes were added. Also the frequency of bit errors would dramatically increase if the file lost synchronization before all bytes of the file were transmitted.

Table A.3 shows the BER results using different criteria to judge when a bit error occurred. Each criterium is defined below.

**Raw BER** The raw bit error rate is the most sound criterion for bit errors. These errors were tallied during normal operation of the transmission for ASCII bytes that were changed to another byte with a flip of a bit or two or three.

**1 Error From Last Line (1 Last)** This criterion only counted one error from the last line of transmission when one or more were present. Since the frequency of errors increased due to loss of synchronization, a controlled bit error count was desired.

**All Errors from Last Line (All Last)** All bit errors were counted in last lines up to end of received data. Totally erroneous data that occasionally was observed at lost synchronization was ignored.

**One Error for Deleted Blocks and Added Bytes (1 from add and delete)** Each contiguous block of deleted bytes was counted as one error and each added byte was counted as one bit error. It was assumed that a bit in the transmitted frame overhead flipped causing these types of errors. Since the framing bits were not calculated in the BER calculations used for the final results, this criterion was not used.

*A.2.3 Normality of BER Measurements.* This section presents methods that test how well the data from the BER measurements satisfy the conditions

Table A.3 BER results using various criteria.

Criteria	All Transmitted Bits (No Stop Bits)			All Transmitted Bits with Stop Bits			Transmitted Bits with Deleted Bits Subtracted (No Stop Bits)		
	4dB	5dB	6dB	4dB	5dB	6dB	4dB	5dB	6dB
Raw BER	7.6663E-05	1.2079E-05	3.5264E-06	6.8145E-05	1.0737E-05	3.1346E-06	7.6858E-05	1.2086E-05	2.5191E-06
Raw BER w/ 1 error from last line	9.5311E-05	1.3938E-05	3.5264E-06	8.4721E-05	1.2389E-05	3.1346E-06	9.5553E-05	1.3946E-05	3.5267E-06
Raw BER w/ all errors from last line	0.00016369	1.4867E-05	3.5264E-06	0.0001455	1.3215E-05	3.1346E-06	0.0001641	1.4876E-05	3.5267E-06
One last and 1 from Add and delete	0.00012225	2.2301E-05	4.534E-06	0.00010866	1.9823E-05	4.0302E-06	0.00012256	2.2313E-05	4.5343E-06
All last and 1 from Add and delete	0.00019062	2.323E-05	4.534E-06	0.00016944	2.0649E-05	4.0302E-06	0.00019111	2.3243E-05	4.5343E-06

needed for accurate ANOVA. These assumptions were made in order to perform ANOVA on the data.

1. The effects of various factors are additive.
2. Errors are additive.
3. Errors are independent of the factor levels.
4. Errors are normally distributed.
5. Errors have the same variance for all factor levels.

[Jai91] recommends preparing a residual versus predicted response plot to verify independence of errors and a normal quantile-quantile plot to verify that the residuals are normally distributed.

A normal quantile-quantile plot is shown in Figure A.3(a) for the ANOVA on the BER measurements presented in Chapter IV. The  $R^2$  value for the data is just above 0.80, which is the minimum acceptable value to declare the residuals normally distributed. Figure A.3(b) shows no real trend in the residuals versus predicted response plot which indicates that the errors are independent of the factors.

The data would probably behave better if the trial sizes were larger, eliminating the numerous zero values recorded. Similar plots were made for a subset of data to

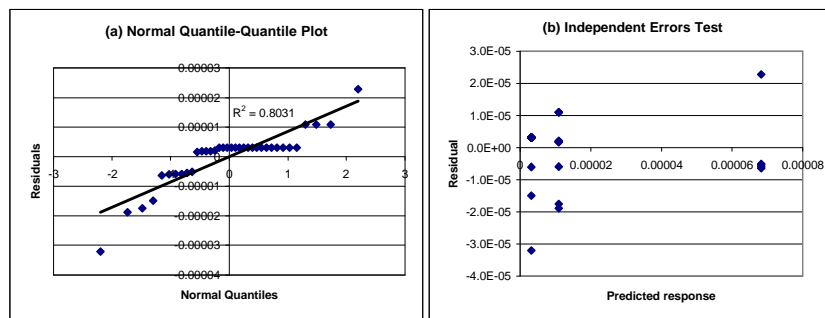


Figure A.3 (a) Quantile-Quantile Plot for ANOVA normality test, (b) Residual versus Predicted Response for ANOVA independence of errors test.

test the assumptions on the non-zero responses. This test produced a much better  $R^2$  value, 0.93, in the quantile-quantile plot supporting the assumption of normality. Figure A.4 shows the quantile-quantile plot for this subset of data.

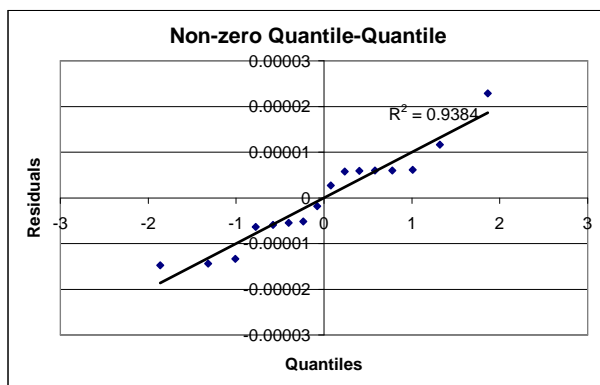


Figure A.4 Non-zero Quantile-Quantile Plot for ANOVA normality test.

### A.3 Summary

This appendix presented detailed and complementary data for the two experiments discussed in Chapter IV. It also presented visual tests on the assumptions made for the ANOVA on the BER measurements.



## *Appendix B. Hardware*

This appendix describes the hardware used for the test bed setup and the attenuation measurements.

### *B.1 Waveplex Spread Spectrum Development Board*

The Waveplex spread spectrum chip set contains a fully functional spread spectrum transceiver. The core of the chip set is the SX043 spread spectrum baseband processor and the SX061 QPSK/BPSK demodulator. The SX043 will simultaneously transmit and receive spread spectrum signals. Different attributes for various board operational modes are set in these two chips via a microcontroller. The microcontroller is given commands via a serial connection to a personal computer terminal program. The board also contains IF circuitry that allows loop-back operation used in this research. The board is shown in Figure B.1 [Wav98].

A problem encountered with this board was that the maximum file transmission size was limited by an internal FIFO buffer in the microcontroller. The FIFO controls the incoming and outgoing datastream on the receive and the transmit side of the system. This current version of the board would cause overflow if too large a file was sent. An overflow would result in loss of data. The size of the buffer was not attainable. It was found that a file of 2049 characters would pass without loss of data due to overflow of this buffer [Wav98].

The global functionality of the board is shown in Figure B.2. The outgoing data is spread by the SX043 which creates the TX-I and TX-Q signals that are modulated on the IF carrier and passed to the IF-out connector. Reception of the signal begins with despreading of the incoming signal. The data signal is passed through a band pass filter and amplified by the auto gain control (AGC) amplifier. The AGC signal is created by the AGC output of the SX061 demodulator then amplified by an integrator. The SX061 demodulates the signal and passes the data

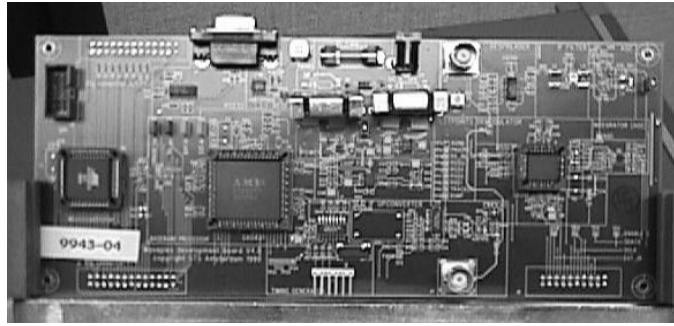


Figure B.1 Waveplex Spread Spectrum Development Board

and a received signal strength indicator (RSSI) to the SX043. The RSSI signal allows the SX043 to perform synchronization and code tracking for the incoming signal [Wav98] [AMI61].

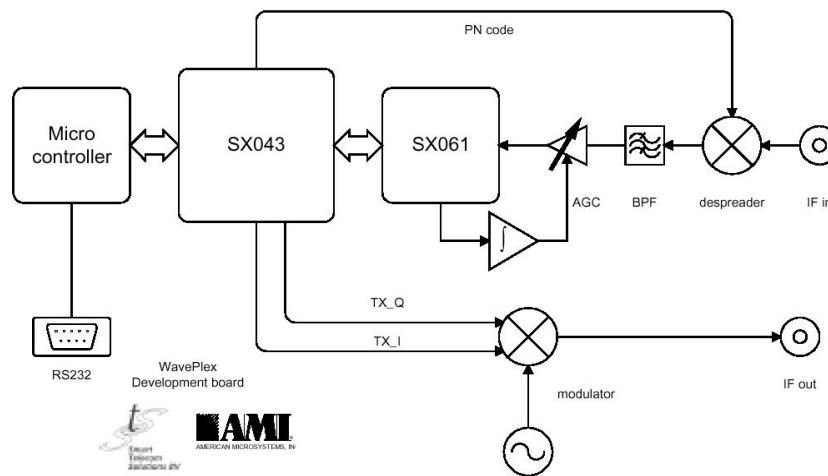


Figure B.2 Waveplex Development Board Functional Diagram

The SX043 provides the spread spectrum operation of the board including PN sequence generation, data spreading and tracking of the incoming signal. The SX043 operation is dictated through internal registers with inputs sent through the microcontroller. The SX043 receives outgoing data into a first-in first-out (FIFO) transmit buffer. In packet mode, it then packages the data into a frame consisting of an adjustable length preamble, 2 byte preamble end code, 8 bit start flag, 16 bits of receive addresses, all data in the FIFO buffer, a 16 or 32 bit cyclic redundancy code

and an 8 bit end flag. In non-packet mode the preamble is immediately followed by data and, when the transmit FIFO is empty, the end flag is sent [AMI43]. This research used packet mode. Only the data is considered in BER calculations.

The bits are then spread by a configurable PN sequence with up to 64 MHz chipping rate. The SX043 is capable of generating maximal length, Gold, and Barker codes with code lengths of up to 2047 bits. Each code is configured by adjusting the maximal length taps and in the case of Gold codes, an offset for the second m-sequence generator to produce  $2^n - 1$  Gold code sequences [AMI43].

The SX043 receives data using an acquisition and track methodology. Acquisition is performed with two states, “sync” and “slip”. The “sync” state establishes the RSSI voltage level used as the reference level for zero correlation between the receiver’s PN code and the incoming PN code. The “slip” state begins once the RSSI level is established [AMI43].

The “slip” state examines the RSSI for a specified time period. If a correlation flash has not occurred the receiver’s PN clock is delayed by successive slips, until correlation occurs. When a correlation flash occurs between the receiver’s PN code and the incoming PN code, the receiver switches to track mode [AMI43].

In track mode a tau-dither tracking loop is used. The tracking loop generates dither error signals by increasing and decreasing the phase of the PN clock by 20%. This creates small variations in the correlation and causes the loop to continually correct itself and approach perfect correlation [AMI43].

## B.2 MFJ Cable Analyzer

The MFJ-269 HF/VHF/UHF Standing Wave Ratio (SWR) analyzer, shown in Figure B.3, is a compact Radio Frequency impedance analyzer. It is referred to as a *cable analyzer* for this thesis. It provides measurements of impedance including resistance and reactance, standing wave ratio and cable loss for coaxial transmission lines. In order to measure loss of a coaxial cable, the opposite end of the cable under

test must be an open circuit (no termination). The unit supports frequencies of 1.8 - 170 MHz and 415-470 MHz. It displays the coax loss in dB at any frequency it supports. The analyzer's provided connector is a N female connector. A Male-N to Female-UHF connector converter is also provided. Finally, a Male-UHF to BNC connector converter was used to attach the 10Base2 cable [MFJ99]. Unreliable



Figure B.3 MFJ-269 Cable Analyzer

readings can occur from the following areas [MFJ99]:

1. Signal ingress from external voltage sources.
2. Diode detector and A/D converter errors.
3. The impedance of connectors, connections, and connecting leads.

### B.3 New Wave LRS-100 Spread Spectrum Generator

The LRS-100 was used to produce the PN sequence for the multiple access interference of the DS/CDMA LAN test bed. The PN sequence generator is highly customizable and allows BPSK, QPSK and staggered QPSK modulation of the sequence. The sequences are configurable by varying 2 to 16 stages of a high-speed shift register with linear feedback. These stages coincide with the taps referred to in Chapters 3 and 4. Each frequency can be externally clocked such as the data rate and the PN sequence rate, or chipping rate. Figure B.4 shows the LRS-100 [New98].

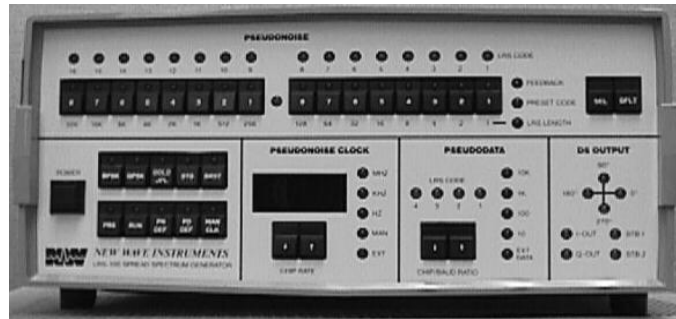


Figure B.4 LRS-100 Spread Spectrum Generator

### B.4 Hewlett Packard 8568B Spectrum Analyzer

The HP spectrum analyzer was used to measure attenuation from the 10Base-2 cable. It was used to measure total average power of the MAI and the SOI. It was also used in validation of measurements and in comparing chipping rates of the interference source and Waveplex SS transmitter in experiment 2. The HP spectrum analyzer is displayed in Figure B.5

The spectrum analyzer is capable of analyzing frequencies between 100Hz to 1.5GHz. It allows multiple display options such as linear display, millivolts per Hz, or logarithmic display which displays decibels with reference to 1 milliwatt or dBm per Hz. The analyzer allows for detailed measurements using zoom features and a marker which identifies the observed frequency and power (or voltage) [HeP68].



Figure B.5 HP 8568B Spectrum Analyzer

### *B.5 Hewlett Packard 8645A Agile Function Generator*

The HP function generator provided the IF frequency and power level for the MAI signal. It produced the 5 MHz that was mixed with the output of the PN sequence generator for experiment 2. The HP function generator allowed variable power levels of the 5 MHz signal. The variable amplitude of the signal enabled the MAI signal to be increased to a level that, when attenuated with the step attenuator, would provide adequate interference. It is shown in Figure B.6.



Figure B.6 HP 8645A Agile Function Generator

### *B.6 Auxiliary Hardware*

Numerous supporting hardware were used for this research. Equipment used to simulate the MAI signal also included the Tektronix FG502 11MHz Function Generator, which produced the external chipping rate for the LRS-100 PN sequence

generator. Figure B.7 shows a (a) Telonic, Incorporated step attenuator was used to linearly vary the signal power from the mixed MAI signal created by the hardware discussed above; a (b) Mini circuits ZAD-1-1 well balanced mixer and a (c) Mini Circuits ZFRSC-2050 power splitter. An SC504 80MHz Oscilloscope was also used to make miscellaneous supporting measurements.

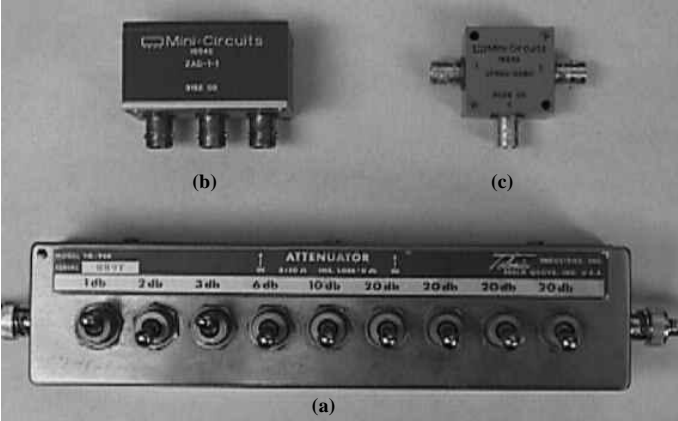


Figure B.7 (a) Telonic step attenuator. (b) Mini-Circuits well balanced mixer and (c) power splitter.

## *Appendix C. OPNET*

This appendix gives a brief overview of Optimum Performance NETWORK Modeler (OPNET). It presents the default pipeline stages OPNET provides to model communications between bus and radio transmitters. After the default radio and bus pipelines are described, the DS/CDMA bus pipeline stages used for this research are summarized.

### *C.1 OPNET Overview*

OPNET is a powerful network simulation development tool. It uses discrete time event simulation to track numerous packets of simulated data through the designed network. Design of network simulation is broken into three domains. These three domains and the OPNET kernel, which provides a myriad of functional capabilities, allow network designers freedom in describing and analyzing network functionality [MIL97].

- The Network domain describes how multiple users or *nodes* are interconnected in some defined universe. The network domain defines the topology of the network.
- The Node domain describes a node and how it handles information it receives and transmits. A node may describe network entities as user terminals or workstations, routers, satellites, bridges, mainframes, file servers, etc. Internal to the node is the node model which defines the operation of the node and how it communicates. The node model contains processor modules that process data, queue modules that organize data and communication modules that transmit and receive to and from other nodes in the network.
- The Process domain lies under the node domain. It contains the actual programming code that manipulates the information contained in packets that the node receives.



## C.2 Default Pipeline Stages

There are three types of communication links represented in OPNET, the point-to-point, bus, and wireless (radio) links. All three reside in the node domain. The communication properties of the links are implemented in OPNET by the transceiver pipeline. The transceiver pipeline is a series of stages that perform calculations on the packets being transmitted or received. Each transceiver pipeline has a different number of stages that are required to model effects of different media and various link properties. For instance, packets must be duplicated and stages repeated broadcast media. The default radio and bus transceiver pipelines were both adapted for this research. The radio pipeline is summarized below because the DS/CDMA bus transceiver pipeline is comprised of a conglomeration of its various stages.

*C.2.1 Radio Link Transceiver Pipeline.* The radio transceiver pipeline has 14 stages. They are illustrated in Figure C.1. Each stage is summarized below [MIL97].

**Receiver Group - Stage 0** The receiver group stage produces a list of potential transmitter receiver pairs at the beginning of the simulation to dictate which pairs can feasibly communicate.

**Transmission Delay - Stage 1** The transmission delay for the packet is calculated at the time of transmission. It is used for end-to-end delay calculations. This stage need only be calculated once no matter how many nodes are potentially receiving the transmitted packet. After this stage the packet is duplicated for each receiver and the following pipeline stages are calculated for each duplication.

**Link Closure - Stage 2** This stage calculates which communication links satisfy requirements deemed necessary for successful transmission. It is calculated at time of transmission for each packet transmission.

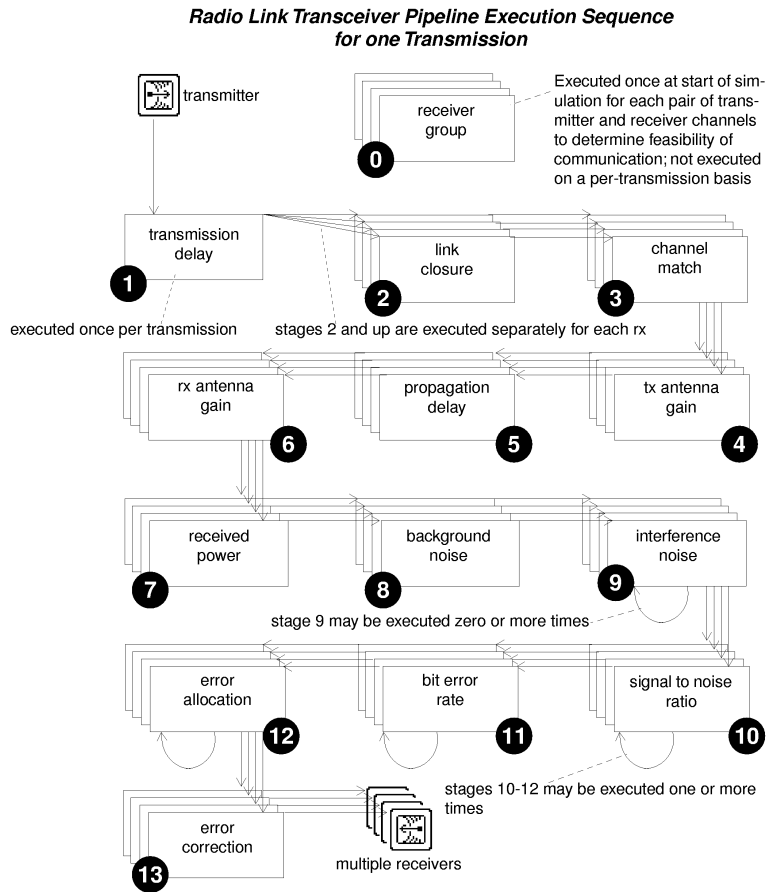


Figure C.1 Radio Link Transceiver Pipeline Execution Sequence for One Transmission [MIL97]

**Channel Match - Stage 3** The properties of the transmitter and receiver, such as frequency bandwidth, data rate, modulation and spreading code, are compared in this stage. Depending on the results of this calculation the stage sets the packet match attribute to valid, noise or ignore.

**RX Antenna Gain - Stage 4** This stage calculates the position of the receiver antenna and computes antenna gain. Since antennas are not used, this stage is not regarded in the DS/CDMA bus pipeline.

**Propagation Delay - Stage 5** Stage 5 computes the distance between antennas and then calculates the delay depending on the transmission medium.

**TX Antenna Gain - Stage 6** Similar to RX antenna gain, this stage computes the location of the receiver relative to the center of the transmitter in order to calculate how much power it receives. Again, this is not used in the DS/CDMA bus since antennas are not used.

**Received Power - Stage 7** The received power stage takes into account the antenna gains and the propagation attenuation and then calculates the received signal power.

**Background Noise - Stage 8** This stage computes the white gaussian noise present in the transmission medium and then sets the noise attribute of the packet. This is the last stage to be calculated at time of packet transmission.

**Interference Noise - Stage 9** This stage calculates noise created by interfering packets during propagation. If the interfering packet's channel match attribute is set to valid or noise then its power will be added to the packet of interest. The noise level for the interfering packet is also adjusted. Whichever packet is out in the medium first is deemed the *previous* packet. The packet beginning reception during reception of a *previous* packet is deemed the *arriving* packet. One or both of the packets must be valid for this stage to occur. This stage can be repeated zero or more times depending on the number of interfering packets. It occurs at time of reception for the *previous* packet. When the interference stage is called the packet is effectively broken into packet segments in which different SNRs and BERs are calculated separately.

**Signal-to-Noise Ratio - Stage 10** This stage calculates the SNR for each packet segment and is repeated one or more times depending on the number of interferers. It is combined with the bit-error-rate stage and the error-allocation in an iteration set. The iteration must complete before any stage repeats. The SNR stage divides the received power by the noise calculated in the interference noise stage. This stage occurs after all the interference stages have been

completed and the packet is fully segmented. The OPNET kernel adjusts the noise level for each segment and each repetition of the SNR stage.

**Bit Error Rate - Stage 11** The BER is calculated here for the packet segment.

The segment length is defined by subtracting the current simulation time by the last SNR calculation time and then multiplying by the data rate.

**Error Allocation - Stage 12** This stage uses the BER calculated in stage 11 and increments the packet's bit error counter using probabilistic methods.

**Error Correction - Stage 13** In the default radio pipeline this stage simply compares the number of bit errors to a designated threshold and decides whether the packet is accepted or rejected.

*C.2.2 Bus Link Transceiver Pipeline.* Unlike the radio pipeline, the bus pipeline only contains six stages. There are many differences in how the link properties are managed between the bus and radio links. The default bus link does not have antenna computations, channel matching or received power computations, nor does it have SNR or BER calculations. The bus link BER is defined as a constant performance rating in the network domain bus link attributes. The bus link can support channels but the channels are modeled as separate wires with no interference between them. Figure C.2 shows the bus link transceiver pipeline. Some stages perform the same basic function such as transmission delay and propagation delay, however they invoke slightly different methods to calculate their data. Since the bus transceiver pipeline does not require as many calculations as the radio model, many transmission data attributes (TDA), present in the radio packet, are omitted from the bus packet. The TDAs describe certain parameters of the transmission properties and are attached to each packet. They are retrieved and operated on within the pipeline [MIL97].

The chief difference between the pipelines, with regards to the goals of this research, is in the collision stage. As shown in Figure C.2, the collision stage is the

**Bus Link Transceiver Pipeline Execution Sequence  
for one Transmission**

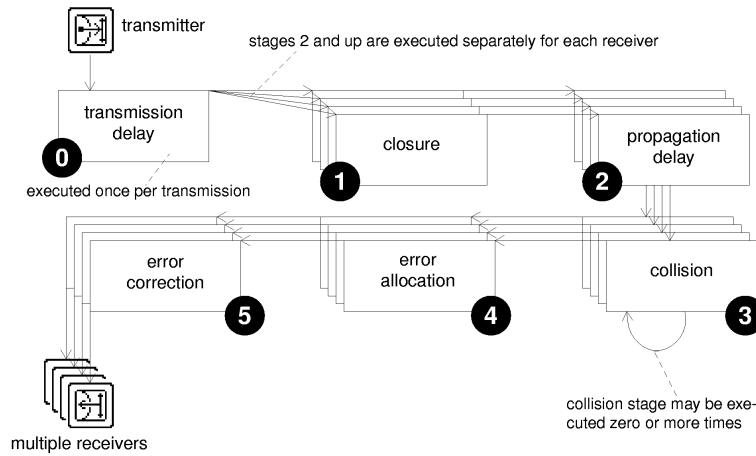


Figure C.2 Bus Link Transceiver Pipeline Execution Sequence for One Transmission [MIL97]

only repeating stage in the bus pipeline. Furthermore, the pipeline assumed that any collision deemed the packet invalid and non-receivable. The rest of the stages are comparable to their radio transceiver pipeline counterparts.

### C.3 DS/CDMA bus pipeline

The DS/CDMA bus pipeline was created by condensing a spread spectrum signalling version of the 14 stage radio pipeline (created by [Bon01]) into a 6 stage bus transceiver pipeline. The bus pipeline was used in order to utilize the bus modelling characteristics in the OPNET *Network* domain design. The most significant alterations are described in Section 3.12.1. The rest of the alterations that created a DS/CDMA bus pipeline are summarized here. The C code for the DS/CDMA bus transceiver pipeline is contained on the CDROM submitted with this thesis [Rap02].

**Transmission Delay - Stage 0** The essence of this stage remains intact from the default pipeline, however, additional TDAs for the transmitter are created and assigned here for the more complex computations needed for a SS bus implementation.

**Closure and Channel Match - Stage 1** This stage combines the SS implementations of the same names. The closure stage portion remains intact — all modelled receivers are eligible for reception. Similar to the closure stage of the radio model described above, it is in this stage that the packets are duplicated for the multiple receivers on the bus. Thus, it is possible to assign the necessary transmission data attributes for the created receiver-specific packets. The channel match stage of the SS implementation is added here in order to assign match categories (valid, noise, ignore) to the duplicated packets. The channel match portion sets up the ability to use multiple channels that interact on the single bus. A packet is valid if its spreading code, modulation, frequency bandwidth, data rate and code family matches the receivers.

**Propagation Delay and Received Power - Stage 2** This stage computes the propagation delay by calculating the distance between transmitter and receiver over the bus and setting the appropriate TDA. Next, the power received by the receiver is computed by attenuating the transmitted power by the cable attenuation calculation. Background noise is also calculated here and set in the packet's TDA. Since the medium is a well shielded copper wire, a very small ambient temperature is used. The first SNR calculation for the following packet segment is calculated here so that a SNR calculation time is recorded to determine packet segment size in the next stage.

**Multiple Access Interference, SNR, BER and Error Allocation - Stage 3** Since this is the only stage that repeats, all of the repeating stages used in the default radio and SS pipelines are incorporated. The BER and Error allocation calculations occur before SNR for they operate on the previous packet segment, while the SNR operates on the next packet segment. Since all packets on the default bus pipeline are assumed to be valid, a conditional statement was added to make sure at least one of the two packets involved in this stage was valid so that the SNR, BER and Error allocation was only performed on

the valid packet(s). The noise accumulation operations are similar to those described above in the default radio pipeline. SS properties are applied and interference calculations are added to the noise accumulation. Further details of this stage's operation were described in Section 3.12.1

**Final BER and Error Allocation - Stage 4** This stage performs the final BER calculations for the last (or only) packet segment and allocates the final errors. Again, this stage is only performed on valid packets so a conditional statement ensuring this is added.

**Error Correction - Stage 5** Like the default radio and bus pipeline stage of the same name there is no error correction algorithms currently present in this stage. It does however, determine whether the packet is accepted by the receiver. The packet is only accepted if it is deemed valid by the channel match stage, does not exceed set threshold of bit errors and the receiving node has not failed.

Another pseudo-stage, *Scheduled End of Interference Event*, was added as described in Section 3.12.1. It performs a BER calculation, allocates errors, and calculates the next packet segment's SNR if a noise packet ends transmission before an concurrent valid packet. The interference caused by the noise packet exiting the channel is decremented in this stage before calculating the new SNR. In the default radio pipeline, the noise accumulation was decremented automatically by the OPNET kernel.

#### *C.4 Packet Trace Verification*

In order to verify that the DS/CDMA bus model functioned properly, the stages involved in calculating BER, SNR and allocating errors were examined. A packet trace was observed on two packets whose matches were *valid* and *noise*. The noise packet was smaller than the valid packet so it began and ended transmission while the valid packet was being received — a case similar to the example given in

Figure 3.3. Figure C.3 displays a portion of a packet trace for the two packets. Only the relevant trace information is shown, breaks from the original trace are shown with ~'s. The packet trace only shows OPNET function calls involving packets, so no computational code is displayed. Also, only the interference stage and the scheduled end of interference event are shown. Verification was performed on the rest of the stages in a similar manner. Validation efforts described in Chapter 4 also support the correctness of the rest of the model. Below are the item numbers shown

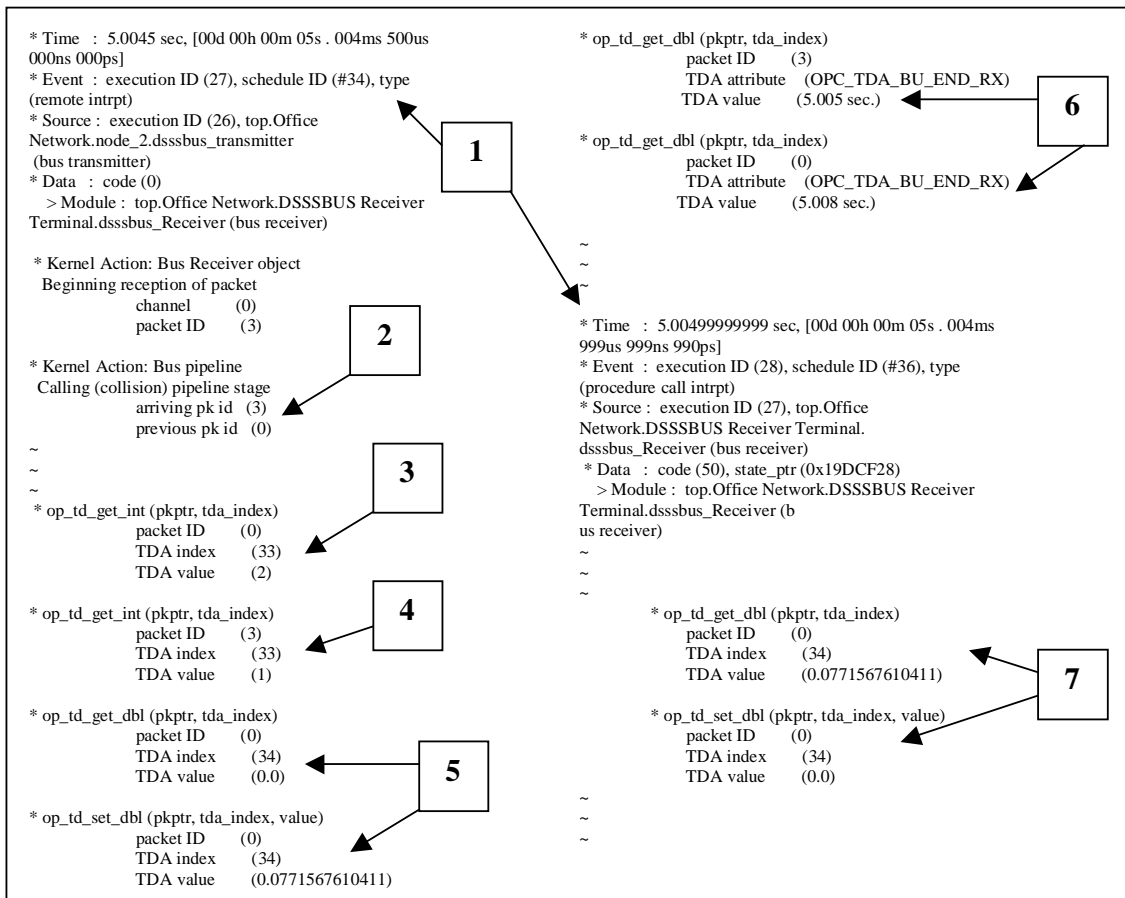


Figure C.3 Packet Trace for Verification of DS/CDMA Bus Model

in Figure C.3:

1. The beginnings of two different discrete events within the simulation are described here, including current time, what object called the event and the



events' identification numbers. The first event, shown to the left of the figure, is the beginning of reception of a noise packet, with packet ID# 3.

2. Item 2 shows that the event called in Item 1 caused the collision pipeline stage to be called. This item also shows that packet ID# 0 was *previously* being received while packet ID# 3 is *arriving*.
3. The function call here retrieves the match status, TDA index 33, for packet ID# 0. The value 2, a representative constant, means that packet 0 is a valid packet.
4. This function call retrieves the match status for packet 3 as 1 or a noise packet.
5. Item 5 displays the incrementing of the noise accumulation, TDA index 34, value for the valid packet 0. Recall that the noise accumulation is calculated by the interfering power from the noise packet 3, 0.0772.
6. Item 6 shows function calls that retrieve the end of reception times for packet 3 and packet 0. The end reception times are compared and if the noise packet 3 ends reception before the valid packet, the noise accumulation set in item 5 must be decremented so that an accurate BER calculation can be accomplished on the non-interfered tail of the valid packet 0. In this case, packet 3 ends reception before packet 0 and an event is scheduled at packet 3's end of reception to decrement the noise and calculate the BER for the interfered segment.
7. Item 7 occurs in the scheduled event mentioned above and shows a function call to retrieve the noise accumulation for packet 0 and decrement it by the noise value of packet 3 since it ended reception.

### *C.5 Summary*

This appendix gave a brief overview of OPNET and its transceiver pipelines for the radio and bus communication links. It described how these pipelines and

the SS radio pipeline devised by [Bon01] were incorporated and modified for a bus implementation of a DS/CDMA LAN. It also verified that the functionality of the newly designed transceiver pipeline used in this research.

## Appendix D. Setting 6 Analysis

This section presents analysis on the 3dB bandwidth of setting 6. It shows that the 3dB measurements made on setting 6 were not reliable as described in Section 4.1.3. A theoretical approximation of the 3dB bandwidth is found for the setting and compared to the measured 3dB bandwidth.

The general shape of a single-sided power spectral density,  $G_x(f)$  for digital data is

$$G_x(f) = T \text{sinc}^2(f - f_c)T \quad (\text{D.1})$$

where  $f$  is all frequencies,  $f_c$  is the carrier wave frequency and  $T$  is the pulse duration.

For setting 6, which is a spread spectrum signal,  $T$  is replaced by the chip duration,  $T_c$ . To find the 3dB bandwidth, or the half-power bandwidth, (D.1) is set equal to  $\frac{T_c}{2}$ . After substituting  $x$  for the argument, as shown in (D.2) we can solve for  $x$  by graphing the  $\text{sinc}^2(x)$  function and finding the  $x$  value where the function value equals  $\frac{1}{2}$ .

$$\text{sinc}^2(x) = \frac{1}{2} \quad (\text{D.2})$$

Using matlab to plot the function,  $x$  was found to be 0.443. Replacing  $x$  by the original argument we have

$$x = (f - f_0) \cdot T_c = \frac{(f - f_0)}{R_c} = \frac{(f - (5\text{MHz}))}{R_c} = 0.443 \quad (\text{D.3})$$

where 5 MHz equals,  $f_0$ , the carrier frequency. With  $R_c$  of setting 6 theoretically equal to 21.3 MHz,  $f$ , solves to 14.4359 which is the frequency that represents the half power point of the spread spectrum, or  $f_{3\text{dB}}$ . The theoretical bandwidth is

$$BW_{3\text{dB}} = 2 \cdot (f_{3\text{dB}} - f_0). \quad (\text{D.4})$$

$BW_{3dB}$  equals 18.9 MHz. However, since part of the spectrum is in negative frequencies, the positive  $BW_{3dB}$  equals 14.9 which is considerably larger than the measured values, 4-6.8 MHz shown in Section 4.1.3. Thus, the measured values are considered inaccurate and setting 6 is dropped from further analysis.

## Bibliography

- [KVM93] C. Mantakas A. Kourtis, C. Vassilopoulos. Evaluation of the number of concurrent users in a baseband cdma lan using statistical analysis. *International Journal of Electronics*, 74(2), 1993.
- [MSS89] C. Smythe A. Marshall, C. Spracklen. An experimental testbed for a direct sequence spread spectrum local area network. In *2nd IEE National Conference on Telecommunications*, 1989.
- [MSS90] C. Smythe A. Marshall, C. Spracklen. Network architectures for a direct sequence spread spectrum lan. In *Proceedings IEEE Symposium of Spread Spectrum Techniques and Applications*, 1990.
- [AMI43] American Microsystems, Inc., 2300 Buckskin Road, Pocatello, ID, 83201. *Spread Spectrum ICs User's Manual*, 1996. Includes the SX063 base band processor.
- [AMI61] American Microsystems, Inc., 2300 Buckskin Road, Pocatello, ID, 83201. *SX061 User's Manual*, 1998.
- [Wav98] American Microsystems, Inc., 2300 Buckskin Road, Pocatello, ID, 83201. *WavePlex Development Board User's Manual*, 1998.
- [Bon01] R. Bonner. Using direct-sequenced spread spectrum in a wired local area network. Master's thesis, Air Force Institute of Technology, March 2001.
- [BoS79] P.O. Borjesso and C.E. Sundberg. Simple approximations of the error function  $q(x)$  for communication applications. *IEEE Transactions on Communications*, COM27:639–642, March 1979.
- [SSS87] M. Scott, C. Spracklen, C. Smythe and N. Ismail. Spreadnet - a spread-spectrum local area network. *Journal of the IERE*, 57(1), Jan/Feb 1987.
- [Dix76] R. C. Dixon. *Spread Spectrum Systems*. Wiley Interscience, New York, 1976.
- [Hay83] S. Haykin. *Communication Systems*. John Wiley and Sons, Inc., New York, NY, 1983.
- [Hel98] G. Held. *Ethernet Networks*. John Wiley and Sons, Inc, New York, NY, 1998.
- [HeP68] Hewlett Packard. *8568B Spectrum Analyzer 100Hz-1.5GHz Operations Manual*.
- [Hol92] J. Holtzman. A simple, accurate method to calculate spread-spectrum multiple-access error probabilities. *IEEE Transactions on Communications*, 40(3), March 1992.

- [IEE85] IEEE. Carrier sense multiple access with collision detection access method and physical layer specifications. *ANSI/IEEE Standard 802.3*, 1985.
- [IEE97] IEEE. Carrier sense multiple access with collision detection access method and physical layer specifications. *ANSI/IEEE Standard 802.11: Wireless LAN Standard*, 1997.
- [Jai91] R. Jain. *The Art of Computer Systems Performance Analysis*. John Wiley and Sons, Inc., New York, 1991.
- [LeP87] J.S. Lehnert and M.B. Pursely. Error probabilities for binary direct-sequence spread spectrum communications with random signatures. *IEEE Transactions on Communications*, COM-35:87–89, 1987.
- [MiA95] J.S. Milton and J.C. Arnold. *Introduction to Probability and Statistics*. McGraw-Hill, Inc., Boston, Massachusetts, third edition, 1995.
- [MFJ99] MFJ Enterprises, Inc., 300 Industrial Park Road, Starkville MS, 39759. *MFJ HF/VHF/UHF SWR Analyzer, Model MFJ-269*, 1999.
- [GRP00] R. Prodan, M. Grimwood, P. Richardson. Enhancing the docsis cable modem specifications with an advanced physical layer for upstream transmission. *IEEE Digest of Technical Papers*, 2000.
- [MIL97] MIL 3, Inc., 3400 International Drive, NW Washington D.C., 20008. *OP-NET Modeler*, 1997.
- [New98] New Wave Instruments, 3760 Masters Court, San Jose, CA, 95111. *LRS-100 Spread Spectrum Generator*, 1998.
- [Rak97] S. Rakib. An innovative cable modem system for broadband communication. In *International Broadcasting Convention*. IEE, 1997.
- [Rap02] J. Rapallo. Validation of a direct sequenced code division multiple access local area network. CDROM submitted with thesis, March 2002.
- [PZB95] R. Ziemer, R. Peterson and D. Borth. *Introduction to Spread Spectrum Communications*. Prentice Hall, Upper Saddle River, NJ, 1995.
- [RSA78] L. Adleman, R. Rivest, A. Shamir. A method for obtaining digital signatures and public-key cryptosystems. *Communications ACM*, (21), 1978.
- [DES] SAS Institute, Inc. *Federal Standard 1026, Telecommunications: Interoperability and Security Requirements for use of the Data Encryption Standard in Data Communication Systems*.
- [Skl88] B. Sklar. *Digital Communications: Fundamentals and Applications*. Prentice-Hall, Upper Saddle River, New Jersey, 1988.
- [Smy85] C. Smythe. *Direct Sequence Spread Spectrum Techniques in Local Area Networks*. PhD thesis, Durham University, UK, 1985.

- [SpS87] C.T. Spracklen and C. Smythe. Direct sequence spread spectrum access to local area networks. In *IEEE Milcom 87 conference proceedings*, October 19-22 1987.
- [Tan96] A. Tannenbaum. *Computer Networks*. Prentice Hall PTR, Upper Saddle River, NJ, 1996.
- [Tim01] Times Microwave Systems, 358 Hall Ave., Wallingford, CT, 06492-5039. *Complete Coaxial Cable Catalog and Handbook*, April 2001.
- [KPP91] P.A. Perrier W.C. Kwong and P.R. Prucnal. Performance comparison of asynchronous and synchronous code-division multiple-access techniques for fiber-optic local area networks. *IEEE Transactions on Communications*, 39(11), 1991.

## *Vita*

Captain James R. Rapallo Jr. earned his Bachelor of Science in Electrical Engineering from the University of Southern California in Los Angeles. He graduated and was commissioned in May 1997.

His first assignment in the United States Air Force was at the National Air Intelligence Center at Wright-Patterson Air Force Base in Dayton, Ohio. There, he served as a foreign radar systems engineer. In August 2000, he entered graduate studies at the Air Force Institute of Technology also at Wright-Patterson AFB. Upon graduation, he will be assigned to the Air Force Research Lab Munitions directorate at Eglin AFB, Fort Walton Beach Florida.

Permanent address: Air Force Institute Of Technology  
2950 P St.  
Wright-Patterson AFB, OH 45433-7765



REPORT DOCUMENTATION PAGE			Form Approved OMB No. 074-0188		
<p>The public reporting burden for this collection of information is estimated to average 1 hour per response, including the time for reviewing instructions, searching existing data sources, gathering and maintaining the data needed, and completing and reviewing the collection of information. Send comments regarding this burden estimate or any other aspect of the collection of information, including suggestions for reducing this burden to Department of Defense, Washington Headquarters Services, Directorate for Information Operations and Reports (0704-0188), 1215 Jefferson Davis Highway, Suite 1204, Arlington, VA 22202-4302. Respondents should be aware that notwithstanding any other provision of law, no person shall be subject to a penalty for failing to comply with a collection of information if it does not display a currently valid OMB control number.</p> <p><b>PLEASE DO NOT RETURN YOUR FORM TO THE ABOVE ADDRESS.</b></p>					
1. REPORT DATE (DD-MM-YYYY) 15-03-2002		2. REPORT TYPE <b>Master's Thesis</b>		3. DATES COVERED (From – To) Jun 2001 – Mar 2002	
4. TITLE AND SUBTITLE  A DIRECT SEQUENCE CODE DIVISION MULTIPLE ACCESS LOCAL AREA NETWORK MODEL			5a. CONTRACT NUMBER		
			5b. GRANT NUMBER		
			5c. PROGRAM ELEMENT NUMBER		
6. AUTHOR(S)  James R. Rapallo Jr., Captain, USAF			5d. PROJECT NUMBER		
			5e. TASK NUMBER		
			5f. WORK UNIT NUMBER		
7. PERFORMING ORGANIZATION NAMES(S) AND ADDRESS(S) Air Force Institute of Technology Graduate School of Engineering and Management (AFIT/EN) 2950 P Street, Building 640 WPAFB OH 45433-7765			8. PERFORMING ORGANIZATION REPORT NUMBER  AFIT/GE/ENG/02M-22		
9. SPONSORING/MONITORING AGENCY NAME(S) AND ADDRESS(ES) AFCA/ITAI Attn: Mr. Ronald Price 203 West Losey St. Rm 1065 SCOTT AFB, IL 62225			10. SPONSOR/MONITOR'S ACRONYM(S)		
			11. SPONSOR/MONITOR'S REPORT NUMBER(S)		
12. DISTRIBUTION/AVAILABILITY STATEMENT  APPROVED FOR PUBLIC RELEASE; DISTRIBUTION UNLIMITED.					
13. SUPPLEMENTARY NOTES AFIT Technical POC: Major Rusty O. Baldwin, AFIT/ENG rusty.baldwin@afit.edu					
14. ABSTRACT The United States Air Force relies heavily on computer networks for every-day operations. The medium access control (MAC) protocol currently used by most local area (LAN) permits a single station to access the network at a time (e.g. CSMA/CD or Ethernet). This limits network throughput to, at most, the maximum transmission rate of a single node with overhead neglected. Significant delays are observed when a LAN is overloaded by multiple users attempting to access the common medium. In CSMA/CD, collisions are detected and the data sent by the nodes involved are delayed and transmitted at a later time. The retransmission time is determined with a binary exponential back-off algorithm.  Code Division Multiple Access (CDMA) is a technique that increases channel capacity by allowing multiple signals to occupy the same bandwidth simultaneously. Each signal is "spread" through multiplication with a unique pseudo-random code that distinguishes it from all other signals. Upon reception, the signal of interest is "despread" and separated from other incoming signals by multiplying it with the same exact code. With this technique, it is possible for multiple stations to transmit simultaneously with minimal ill effects.  A simulation model is developed for a direct sequence spread spectrum CDMA (DS/CDMA) channel that incorporates the effects of multiple access interferers (MAI) having spreading codes from the same or different code families. The model introduces cross-correlation coefficients to calculate the signal-to-interference ratio and determine channel bit error performance. Transmission media attenuation and the near-far effects are accounted for in the model design. The model utility is demonstrated by determining the loss characteristics of a coaxial spread spectrum network. Due to the modular design, other transmission media characteristic can be easily incorporated. A bus network topology is simulated using 10Base2 coaxial cable. The model is compared and validated against a spread spectrum local area network hardware test bed.					
15. SUBJECT TERMS Code Division Multiple Access, Local Area Network, Spread Spectrum, Bus, 10Base-2					
16. SECURITY CLASSIFICATION OF:			17. LIMITATION OF ABSTRACT	18. NUMBER OF PAGES	19a. NAME OF RESPONSIBLE PERSON
a. REPORT	b. ABSTRACT	c. THIS PAGE			Rusty O. Baldwin, Major (ENG)
U	U	U	UU	118	19b. TELEPHONE NUMBER (Include area code) (937) 255-3636, ext 4612; e-mail: rusty.baldwin@afit.edu